



universität
wien

MASTERARBEIT

Titel der Masterarbeit

„Synthese und Charakterisierung neuer Ruthenium-Nitrosyl Komplexe mit
Aminosäuren“

Verfasserin

Anna Rathgeb, BSc

angestrebter akademischer Grad

Master of Science (MSc)

Wien, 2013

Studienkennzahl lt.

A 066 862

Studienblatt:

Studienrichtung lt.

Chemie

Studienblatt:

Betreuer:

ao. Univ.-Prof. Dr. Vladimir Arion



universität
wien

MASTER THESIS

Title

„Synthesis and Characterization of Novel Ruthenium-Nitrosyl Complexes with Amino Acids“

Author

Anna Rathgeb, BSc

intended academic degree

Master of Science (MSc)

Vienna, 2013

Subject: Chemistry

Supervisor: ao. Univ.-Prof. Dr. Vladimir Arion

Acknowledgement

I want to thank all the people who helped me during my master thesis:

O. Univ.-Prof. Dr. Dr. Bernhard K. Keppler for the opportunity to work in his skilled and experienced group.

Ao. Univ.-Prof. Dr. Vladimir Arion for being an excellent and patient supervisor.

Prof. Éva A. Enyedy for her great supervision, the explanations on solution chemistry and the help during my work in Hungary.

Orsolya Dömötör, MSc. for the practical supervision during my work in Hungary.

Mag. Dr. Michael Jakupec and Maria Novak MSc. for performing the cell tests.

Mag. Anatolie Dobrov and Mag. Aliona Luganschi for the ESI MS measurements.

Ao. Univ.-Prof. Mag. Dr. Markus Galanski, Dipl.-Chem. Paul-Steffen Kuhn, Dipl.-Ing. Dr. Wolfgang Kandioller, Dipl.-Ing. Melanie Schmidlehner, Mag. Michael Primik and Mag. Verena Pichler for measuring NMR spectra.

Mag. Johannes Theiner and all members of the microanalytical Laboratory for the elemental analyses.

Mag. Alexander Roller for the X-ray diffraction measurements.

Mag. Elfriede Limberger for her help regarding administrative concerns.

Mihai Odoeanu for the material supplies.

My colleagues Ewelina Orłowska, BSc, Sonja Platzer, BSc and all my colleagues in Docroom2 for the great working atmosphere and all their support.

Zusammenfassung

Seit Cisplatin entdeckt wurde, sind Platin(II) Komplexe ein integraler Bestandteil der anti-Krebs Chemotherapie. Trotz ihrer beachtlichen Wirksamkeit gegen manche Krebsarten, ist die Suche nach Alternativen notwendig, da schwere Nebenwirkungen auftreten und verschiedene Tumore Resistenzen zeigen.

Wie seit mehreren Jahren bekannt ist, sind einige Ruthenium(II) und (III) Verbindungen vielversprechende potentielle Chemotherapeutika, obwohl noch nicht restlos geklärt ist, auf welche Weise sie wirken.

Spätestens seit die anti-angiogenetischen und anti-invasiven Eigenschaften von NAMI-A teilweise auf die Bindung von freiem NO zurückgeführt werden konnten, stellt Nitrosyl einen interessanten Liganden für Chemotherapeutika dar. Nitrosyl spielt im Organismus eine Rolle als Signalmolekül und trägt zur Regulierung des Blutdrucks bei, indem es gefäßerweiternd wirkt. Darüber hinaus wird bei Entzündungsreaktionen, in nekrotischem Gewebe und im Zuge der Apoptose NO freigesetzt. Die Affinität von Ru(II) und (III) zu NO ist in der Literatur gut dokumentiert.

Sowohl im Körper als auch in Zellkulturrexperimenten sind Aminosäuren die wichtigsten kleinen biologischen Liganden. Trotzdem ist wenig über die Reaktivität von Aminosäuren gegenüber Ruthenium-Nitrosylkomplexen bekannt. Ziel unsere Arbeit war diese Lücke zu schließen. Es wurde eine Serie von Ruthenium-Nitrosylkomplexen mit Aminosäure mit der Formel $\text{Bu}_4\text{N}[\text{RuCl}_3\text{NO}(\text{L})]$ (L = L-Ala, L-Val, Gly, L-Ser, L-Thr, L-Tyr, L-Pro, D-Pro) hergestellt und mittels ^1H NMR ESI-MS, UV-vis, ATR-IR Spektroskopie, Cyclovoltammetrie, Elementaranalyse und Röntgenstrukturanalyse charakterisiert. Außerdem wurden Zelltest an drei menschlichen Krebszelllinien durchgeführt, um die IC_{50} Werte zu bestimmen.

$\text{Na}_2[\text{RuCl}_5\text{NO}] \cdot 6\text{H}_2\text{O}$, 1.5 eq Aminosäure und 2 eq Bu_4NCl wurden in *n*-Butanol gelöst und 1.5 Stunden refluxiert. Die Komplexe mit L-Tyr und Gly wurden direkt aus der Mutterlauge kristallisiert. Die übrigen Komplexe wurden aus einer kleinen Menge Wasser kristallisiert.

Abstract

Since the discovery of cisplatin, platinum(II) compounds have become an integral part of anticancer chemotherapy. Despite their remarkable cure rates for some types of cancer, it is necessary to search for alternatives due to the severe side effects of approved platinum compounds and the resistance of some tumor types.

As known for several years ruthenium(II) and ruthenium(III) compounds are promising anti-cancer agents, although the mode of action is still controversial.

At least since the anti-angiogenic and anti-invasive properties of NAMI-A were in part reported to NO capturing, NO, which plays an important role in organism as signaling molecule, in blood pressure regulation, inflammatory response and in necrosis and apoptosis, is an interesting ligand for potential anticancer agents. Moreover ruthenium shows a well described affinity to NO.

Amino acids are the most important biological ligands with low molecular weight in the body as well as in cell culture experiments, nevertheless very little is known about the reactivity of amino acids towards ruthenium-nitrosylcomplexes. We intend to close that gap and therefore a series of ruthenium-nitrosylcomplexes with amino acids, $\text{Bu}_4\text{N}[\text{RuCl}_3\text{NO}(\text{L})]$ (L = L-Ala, L-Val, Gly, L-Ser, L-Thr, L-Tyr, L-Pro, D-Pro), was prepared and characterized by ^1H NMR, ESI MS, UV-vis, ATR IR spectroscopy, cyclic voltammetry, elemental analysis and X-ray crystallography. Furthermore cell culture experiments with three human cancer cell lines were performed. The IC_{50} values were determined.

$\text{Na}_2[\text{RuCl}_5\text{NO}] \cdot 6\text{H}_2\text{O}$, 1.5 eq amino acid and 2 eq Bu_4NCl were dissolved in *n*-butanol and refluxed for 1.5 hours. To obtain the L-Tyr and Gly complexes the *n*-butanol solutions were transferred into a baker. The solutions were filtrated after 24 hours and after several days the desired product crystallized. To obtain the other complexes *n*-butanol was evaporated, the remaining oil was dried *in vacuo* and dissolved in water. Crystals formed after several days.

Table of Contents

1.1 Cancer: Statistics, carcinogenesis and treatment	8
1.1.1 Overview on cancer	8
1.1.2 Carcinogenesis	9
1.1.3 Causes of cancer	12
1.1.5 Overview on therapy	15
1.1.6 Anticancer chemotherapy.....	16
1.2. Metal compounds in anticancer chemotherapy	18
1.2.1 Platinum based drugs	18
1.2.2 Ruthenium in anticancer chemotherapy	20
1.2.3 Modes of action of ruthenium-compounds.....	21
1.2.4 Ruthenium based anticancer drug candidates.....	23
1.3 NO - a noninnocent ligand	25
1.4 α - Amino acids – The smallest biological ligands	27
2.1 Synthesis and characterization of ruthenium-nitrosyl complexes with amino acids	41
2.2 Investigation of the Interaction between HSA and $[\text{MCl}_4\text{NO}(\text{Hind})]^-$ Complexes.....	66

1.1 Cancer: Statistics, carcinogenesis and treatment

1.1.1 Overview on cancer

About 13% of world's population dies from cancer.¹ In Austria and other high income countries cancer is with 26% the second frequent cause of death after cardiovascular diseases.² Figure 1 shows the cumulative risk for both sexes for cancer incidence and mortality to the age of 75 in regions with high and low human development. Due to better health care and hygienic conditions infectious and parasitic diseases are less frequent in highly developed countries. The higher life expectancy leads to a higher risk for cancer. It is also remarkable that different types of cancer occur with variant prevalence in more and less developed regions.

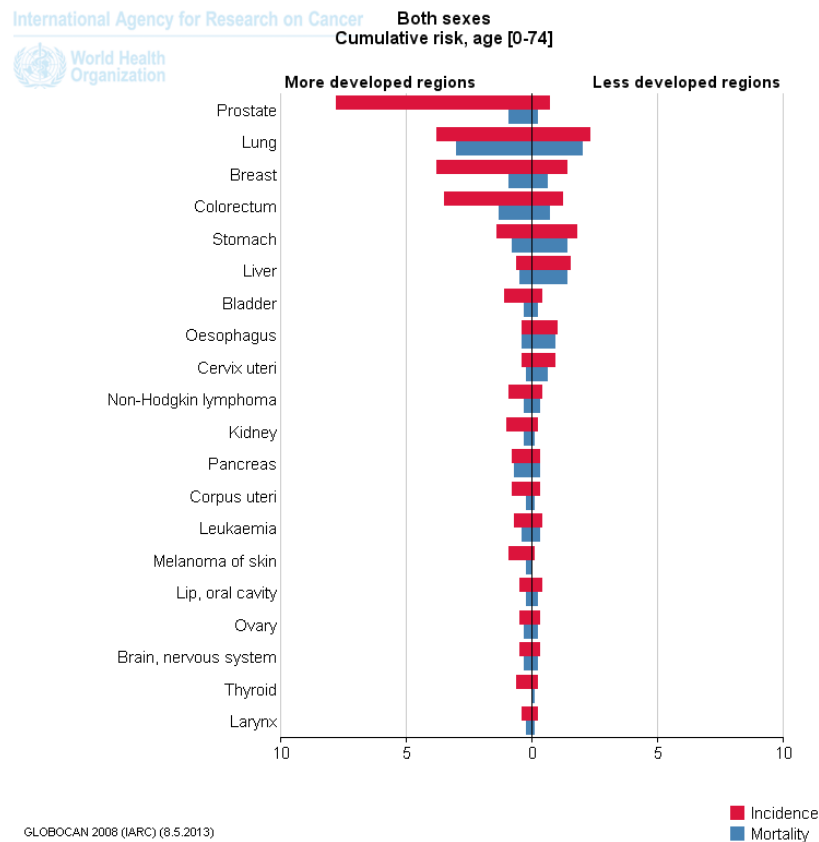


Figure 1. Cumulative risk of cancer incidence and mortality in more and less developed countries.³

In Austria the most common tumor localizations are breast, lung and colon cancer for women and prostate, lung and colon cancer for men (Fig. 2).

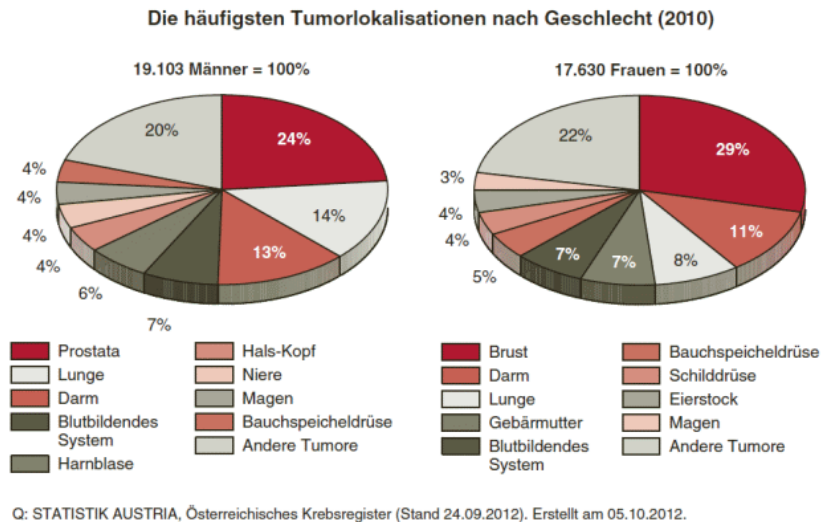


Figure 2. Most common tumor localizations for men and women in Austria.²

1.1.2 Carcinogenesis

Most cell types in a human or animal body carry a complete genome and have the ability to proliferate in an adult organism. This enables the maintenance of tissue and body shape during the whole life, but it also implies the danger that the complicated cell cycle, telling the cell when to rest, to grow, to divide or to die, runs out of control.⁴ Figure 3 shows a schematic view of the cell cycle. It consists of four phases. Two gap phases before and after the DNA synthesis phase, where the cell takes its time to grow and doubles its proteins and organelles and the mitotic phase where the nucleus and finally the whole cell divides.

In G1 phase the cell monitors the external and internal environment and lasts in state G0, the resting phase, if the conditions are unfavorable G1, S and G2 phases together form the interphase. In a typical human cell proliferating culture interphase takes about 23 of 24 hours. Several checkpoints are designed during cell cycle, ensuring that no incomplete or damaged DNA is passed to the daughter cells. Central elements in the cell cycle control are the **cyclin-dependent kinases (Cdks)**.

These enzymes regulate phosphorylation of intracellular proteins, which initiate or regulate significant steps during the cell cycle. Cdks themselves are regulated by a complex array of enzymes and other proteins, the most important of which are the **cyclins** (therefore cyclin depended kinases). Cdks have to be tightly bound to a cyclin to have protein kinase activity. In Figure 3 the Cdks and their cyclins are assigned to the cell cycle phases.

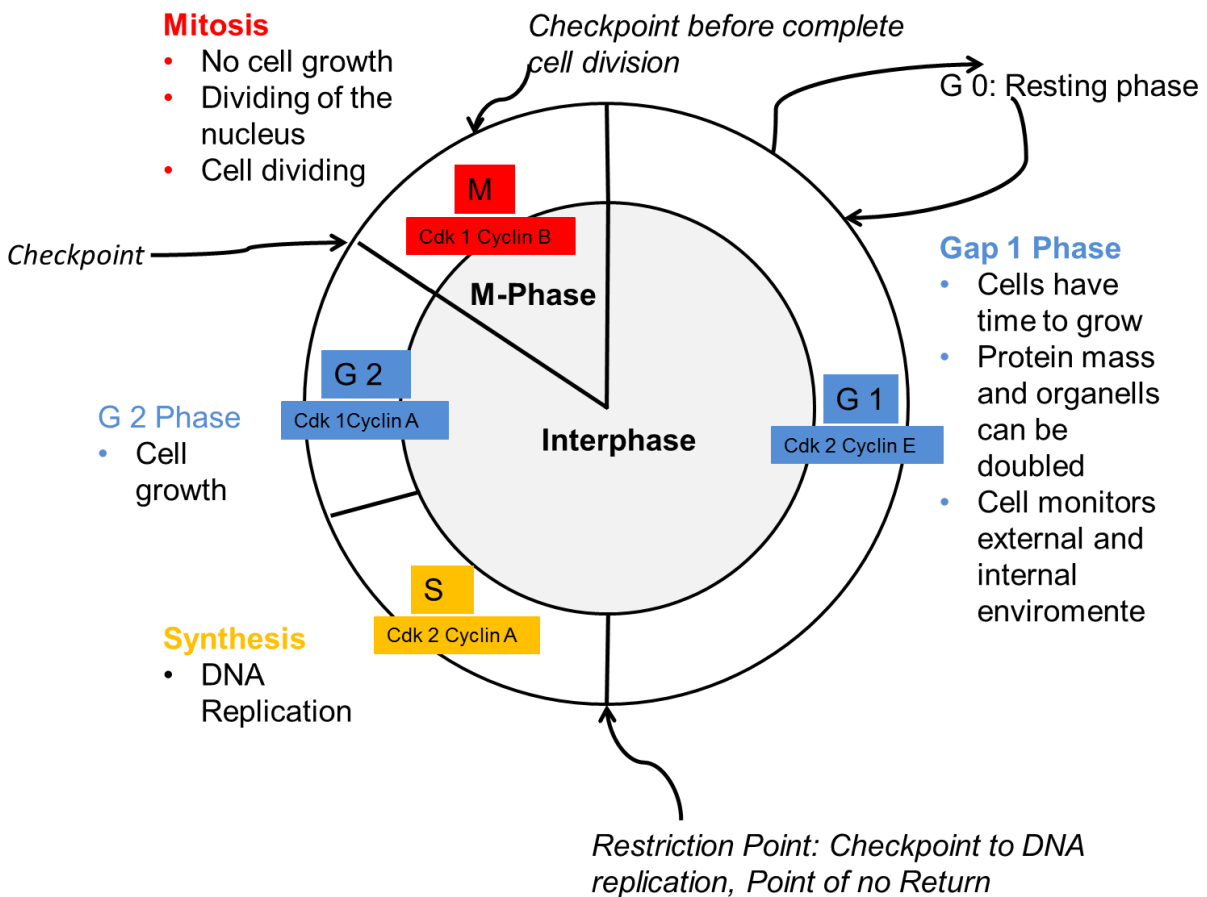


Figure 3 . Schematic drawing of the cell cycle of a typical human cell.

A human body consists of approximately 10^{14} cells, with billions of them mutating every day. Mutations or epigenetic changes (the gene expression changes, not the gene sequence) that give single cells a selective advantage potentially lead to cancer.⁵

Cancer refers to a large group of diseases characterized by unregulated cell proliferation and the ability to invade foreign tissue. Secondary tumor settlements, called metastases, are usually traceable back to the site where they first arose, the primary tumor. Tumor metastases are responsible for about 90% of cancer related deaths.⁴

Cancer cells are genetically unstable, because checkpoint control mechanisms during cell cycle and DNA-repair mechanism often do not work, thus hastens the progression to greater malignancy and can promote resistance against therapy. Human cancer develops over many years, thereby accumulating several independent and rare abnormalities.

Figure 4 illustrates the stages of carcinogenesis. Tumor growth is initiated by a single mutation, this is called tumor **initiation**. The accumulation of mutations while the cells are not yet invasive is termed tumor **promotion**. The resulting invasive cancer starts to spread into foreign tissue; this process is called tumor **progression**.⁵

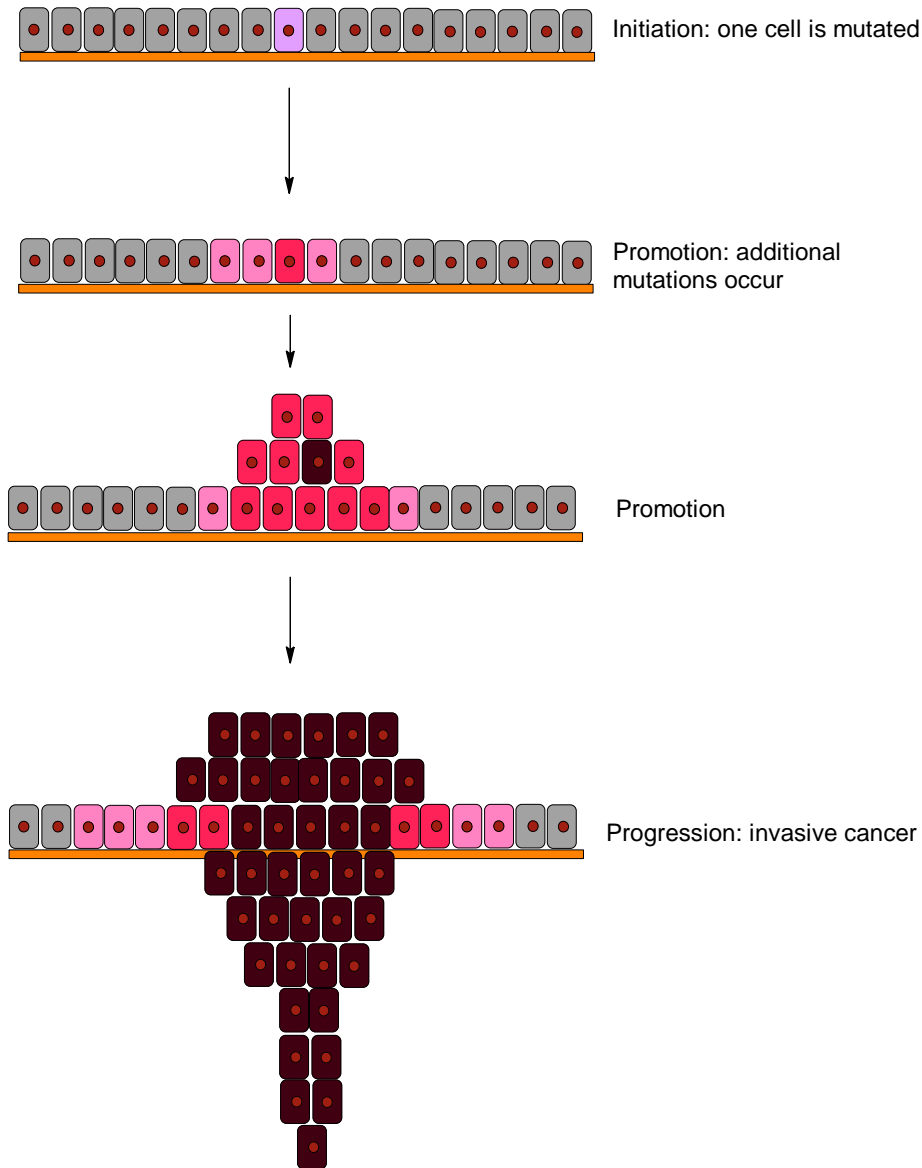


Figure 4 . Illustration of tumor development.

1.1.3 Causes of cancer

As described so far various mutations and epigenetic changes can contribute to the development of cancer. As the accuracy of DNA replication is limited, cancer is a life risk which enhances with age and cannot be completely ruled out. Nevertheless the genetic constitution, environmental conditions and personal lifestyle play an important role in carcinogenesis.

Endogenic causes of cancer

Diverse genes play a crucial role in cancer development. Such genes are classified in three groups, namely **proto-oncogenes**, **tumor-suppressor** and **DNA-maintenance genes**.

Proto-oncogenes

The overexpressed forms of proto-oncogenes are called oncogenes and can drive cells towards cancer. Oncogenes have a dominant genetic effect.⁵ The in the early 1980s first isolated human proto-oncogene *Ras* is mutated in 20% of human cancers. Like most proto-oncogenes, *Ras* plays an important role in stimulating cell proliferation by activating signal transduction pathways, which regulate growth and differentiation processes in the cell. Mutated *Ras* does not respond to external growth signals anymore but stimulates itself.⁶

Tumor-suppressor genes

In the case of tumor suppressor genes a loss of function mutation can lead to cancer. Mutations/epigenetic changes are usually recessive. P53 is an important representative; in nearly all human cancers the gene itself or components of the p53 pathway are mutated. It has manifold role in cell-cycle control, for example by forcing damaged or mutated cells into apoptosis or making them stop dividing until the damage is repaired.⁵

DNA-maintenance genes

The influence of these genes is more indirect. Mutations cause genomic instability.⁵

In some cases cancer can be directly traced back to an inherited gene mutation.

The heritable form of Retinoblastoma is a well-known example for the latter. It occurs in the childhood and is due to a mutation on chromosome 13, the affected child has only one unaffected copy of the gene. If it loses this copy due to a somatic mutation, it will develop the disease.

Environmental factors

Smoking is definitely associated to lung, kidney and bladder cancer. It accounts for ca. 24% of cancer incidence in the western world. It is also known that obesity represents a risk factor.

In general cancer causing agents are called carcinogens. They can be divided into cancer initiators and cancer promoters. Cancer initiators damage the DNA (directly or via their decomposition products)

Typical examples include:

- UV light from sunshine
- Ionizing radiation (as α particles and γ radiation from radioactive decay)
- Aromatic hydrocarbons, amines and nitrosamines
- Alkylating agents such as mustang gas⁵

Tumor promoters are not mutagenic themselves, but they stimulate the proliferation of malignant cells, apparently by inducing an inflammatory response, which leads to an enhanced production of growth factors and proteases. The most widely studied tumor promoters are phorbol esters.⁵

Tobacco smoke contains several mutagen and tumor promoting substances.

Viruses, bacteria and parasites can also cause human cancer. It is estimated that they are responsible for about 15% of human cancer. Especially DNA viruses often carry genes that can cause uncontrolled cell proliferation.

DNA viruses associated to cancer are:

- Papovavirus family (Papillomavirus): benign warts, uterine and cervix carcinoma
- Hepadnavirus family (Hepatitis-B and -C): liver cancer
- Herpesvirus family (Eppstein-Barr virus): Burkitt's lymphoma, nasopharyngeal carcinoma⁴

RNA viruses associated to cancer are:

- Retrovirus family (Human T-cell leukemia virus type I, HIV): adult T-cell leukemia/lymphoma, HIV⁴

1.1.4 Types of human cancer

There are many types of human cancer, but four are the most important:

- Most of the human cancers, namely 85%, are cancers of the epithelia cells, called carcinomas
- Blood cancers are termed leukemia
- Cancers arising from the lymph nodes are called lymphomas
- Sarcomas arise from the connective tissue⁷

1.1.5 Overview on therapy

Nowadays there are three well established strategies to treat cancer:

- surgery
- radiation therapy
- anticancer chemotherapy

Often these therapies are used in combination. Treatment may be administered with a curative intent or to prolong a patient's life. Targeted therapies exploiting the specific abnormalities of a certain type of cancer are still in early stages of development.

Solid tumors that are big enough and operable can be removed by surgery. Surgery is the eldest and up to now still most effective single treatment.

About hundred years ago radiotherapy came up. The tumor can be exposed to irradiation (X-rays, γ -rays) or radionuclides can be accumulated in the tumor tissue by various methods.

Radiation damages the DNA. In case of damage a normal cell would arrest itself until the defects are repaired or undergo apoptosis. Cancer cells often continue to divide and accumulate severe genetic defects, from which they die some days later.⁵

1.1.6 Anticancer chemotherapy

Anticancer chemotherapy implies the treatment of cancer with chemical compounds. The beginnings of chemotherapy reach back to First World War. In 1947 patients suffering from leukemia and lymphoma were treated with nitrogen mustard (a DNA alkylator) and a good but brief response was reported.⁷ Although chemotherapy was developed long before the genetic abnormalities of cancer cells were known, most current cancer therapies work by exploiting these abnormalities.⁵

Classes of chemotherapeutics

According to their mode of action and origin chemotherapeutics can be divided into different classes:

DNA alkylators

Covalent alkyl adducts with the DNA are formed. Adduct formation with two separate bases across the two anti-parallel strands called inter-strand crosslinks and are considered as the most lethal interaction. Tumors with a high fraction of cells in the S phase of the cell cycle are more vulnerable.⁸

Platinum analogues

After cellular uptake, the compounds are activated by hydrolysis and form adducts with the DNA.⁹ For a more detailed description of platinum drugs in clinical application see chapter 2.

Anti-metabolites

Anti-metabolites have structural similarities to certain RNA and DNA precursors and compete with them for binding sites on key enzymes for RNA and DNA synthesis.⁸

Antibiotics

The most widely used antibiotic in chemotherapy is Daunorubicin. Its mode of action is still not understood completely, but seems to include DNA intercalation, free-radical formation, covalent DNA binding and inhibition of the enzyme topoisomerase II.⁸

Plant derived and miscellaneous agents

Many chemotherapeutics used nowadays have originally been isolated from plants or originate from natural substances.⁸ Such phytochemicals show high structural diversity and a general mode of action cannot be postulated.

Topoisomerase I and II inhibitors

The DNA is packed in a compact form, the so called supercoil, if a cell is not dividing. Topoisomerases play an important role in making the DNA accessible for protein machineries and therefore replication.

DNA topoisomerase I and II bind to supercoiled DNA and thereby the DNA relaxes and becomes accessible to replication. Topoisomerase I are monomeric enzymes generating DNA single strand breaks. Topoisomerase II are multimeric enzymes catalyzing DNA double strand breaks. It was discovered in the 1980s that there are drugs, which can inhibit cell proliferation by disturbing the function of the topoisomerases.⁸

1.2. Metal compounds in anticancer chemotherapy

1.2.1 Platinum based drugs

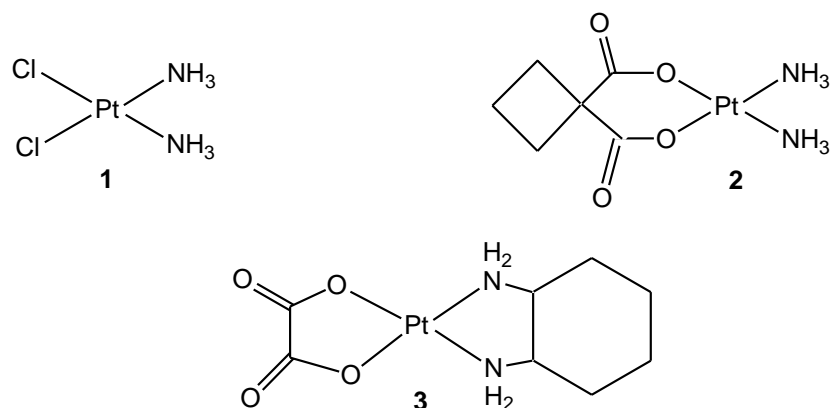


Figure 5. Platinum(II) complexes used in clinical practice. **1:** cisplatin, **2:** carboplatin, **3:** oxaliplatin.

Cisplatin (1)

(SP-4-2)-Diamminedichloridoplatin(II) was first described in 1844 by Michele Peyrone. The anticancer activity of cisplatin was first reported in 1969. It was discovered by Rosenberg *et al.*, who investigated the effect of an electric field on the growth pattern of *E.coli* bacteria. He observed that hydrolysis products of the platinum electrodes, namely Cisplatin and a Pt(IV)-analogue, inhibited cell proliferation.¹⁰

A revolution in cancer therapy followed. Severe side effects of cisplatin including nausea, vomiting and nephrotoxicity, nearly led to studies being discontinued.¹¹ Then it was found out that aggressive diuresis could prevent severe renal damage and further investigations could be undertaken. Antiemetic medicaments were delivered to ease nausea.

Carboplatin (2)

Nevertheless the side effects associated with cisplatin therapy prompted the search for alternatives. It was assumed that introducing more stable leaving groups compared to cisplatin would make the drug more selective to cancer cells and therefore lower the

general toxicity. Carboplatin was developed, which indeed is far less nephrotoxic,¹² but it was found that carboplatin has bone marrow suppression as predominant toxicity.¹³

Cisplatin and Carboplatin turned out to be equivalent in the treatment of ovarian cancer¹⁴ but cisplatin is more effective in testicular, head and neck cancers and therefore remains the preferred treatment for those cancers.¹⁰

The stable amine group which determines the structure of the DNA adduct is identical for cis- and carboplatin, their pattern of tumor sensitivity are in general very similar. Cisplatin or oxaliplatin may have better efficacy in certain tumors, but no tumors are sensitive to carboplatin without responding to one agent or the other cisplatin and vice versa.¹⁰

Oxaliplatin(3)

Platinum(II) complexes with various stable amine groups, especially derivatives of diaminocyclohexane (DACH) were developed in order to broaden the spectrum of anticancer activity. Oxaliplatin was approved in 1998 and is the third platinum analogue with worldwide approval. It has, as can be seen in Figure 5, an unsubstituted diaminocyclohexane ligand. It is more tolerable *in vivo*, its neurotoxicity is dose-limiting.^{15,16,17}

The DNA adducts formed by oxaliplatin were the same as for cis- and carboplatin. Mainly d(GpG)Pt and d(ApG)Pt intrastrand crosslinks are formed¹⁸, but it was showed that oxaliplatin forms fewer crosslinks at equimolar concentrations than cisplatin.¹⁹ The DACH ligand is bulky and hydrophobic and it is hoped that it hinders DNA repair mechanism.

Several tumor cell lines with resistance to cisplatin respond to oxaliplatin²⁰.

Currently oxaliplatin in combination with 5-fluorouracil and folic acid is the preferred method to treat colorectal cancer.²¹

1.2.2 Ruthenium in anticancer chemotherapy

Ruthenium belongs to the transition metal group of the periodic system. It occupies the place below iron and above osmium in group 10. Ru(II) and (III) usually form rather soft complexes. Ruthenium has no known biological function. Some ruthenium complexes are used as catalysts, e.g. the Grubbs catalyst, a ruthenium carben compound, is used in olefin metathesis.²²

The synthetic chemistry of ruthenium is well known, especially its behavior towards amine and imine ligands. The three most common oxidation states, +2, +3 and +4, are available in aqueous solutions and usually were found in octahedral complexes.

Ruthenium amine complexes are promising drug candidates, because reliable synthetic routes leading to stable complexes, which show interesting redox chemistry, have been developed. Profound knowledge of the biological effects of ruthenium complexes has been accumulated.²³

Furthermore, ruthenium has several radioactive isotopes, which are interesting for the development of radiopharmaceuticals.²⁴

Many Ru(II)/(III) amine complexes are capable of selective binding to imine sites in biomolecules and therefore coordination to histidyl on proteins²⁵ and to the *N7* site of purine nucleotides is frequently observed. This behavior enables targeting of specific tissues.²⁶

The known thiolato complexes tend to be kinetically unstable.²⁷ Flavin and pterin complexes are often light sensitive.²⁸

1.2.3 Modes of action of ruthenium-compounds

Activation by reduction hypothesis and DNA binding

Due to the fast growth of tumor cells, latter are characterized by a lower concentration of nutrients and O₂ content (hypoxia) in their surroundings.²⁹ Therefore the metabolism of tumor cells is strongly dependent on glycolysis which leads to an excess of lactic acid and thus lowers the pH (to about 6) in surrounding tissue.³⁰

These differences to normal cells lower the electrochemical potential and should favor the reduction of Ru(III) to Ru(II).

The t_{2g} orbitals in Ru(II) are filled. π-Donor ligands bind less strongly to Ru(II) than to Ru(III). This means that Ru(II) amine complexes loose their acido ligands quite rapidly ($k = 1 - 10 \text{ s}^{-1}$).³¹ Intracellular binding (for example to the DNA) should be promoted, resulting in tumor selective toxicity. The increased DNA binding of [*cis*-Cl₂(NH₃)₄Ru]Cl (CCR) and (ImH)[*trans*-(Im)₂Cl₄Ru] (ICR) has been clearly demonstrated in HeLa cells.³²

Ru(II) is a relatively soft transition metal which binds covalently to the nitrogen sites on the DNA bases, in purine nucleosides most frequently to N7. Beside covalent DNA binding DNA intercalation is also observed, as for example in the case of [Ru(bpy)₂(dppz)]²⁺ and [Ru(phen)₂(dppz)]₂. DNA intercalation of these complexes, with their large, aromatic and planar ligands, markedly enhances luminescence. Thus, the compounds are also interesting as diagnostic tools and not only as therapeutic agents.³³

Several biomolecules as glutathione (GSH), single-electron-transfer proteins or transmembrane electron transport systems can reduce Ru(III) in vivo.³⁴ Ru(II) can be reoxidized to Ru(III) by molecular oxygen, cytochrom c oxidase or other oxidants³⁵ but this is less probable in the hypoxic environment of a tumor.

Transferrin and HSA binding

The interactions of anti-cancer compounds with proteins are of crucial interest, because these interactions influence biodistribution, toxicity and may even the mode of action.

In the blood ruthenium amine and imine complexes are usually bound noncovalently to highly abundant serum proteins such as to human serum albumin (HSA) and transferrin.³⁶ HSA occurs with a concentration up to 630 μM in the blood and is therefore the most abundant blood serum protein. It serves as a transport vehicle for many biological ligands including fatty acids, bilirubin, steroids, metal ions and several pharmaceuticals. It consist of a single chain with 585 amino acids organized in three similar subdomains, with two subdomains each (A and B). The principal regions of the ligand binding sites are located in hydrophobic cavities in subdomains IIA and IIIA (sites I and II).³⁷

The glycoprotein transferrin has a molecular mass about 80 kDa. It consists of a polypeptide chain containing 679 amino acids. The chain is arranged in two similar lobes, each of them able to bind Fe(III). Fe(III) is bound via two tyrosines, one histidine and an aspartate and a bidentate carbonate.³⁸ At pH 6 (as in the surrounding of a tumor) Fe(III) is released. Ru(III) and Fe(III) have similar properties and therefore Ru(III) is able to bind to transferrin. The binding seems to facilitate its entry into the cells.³⁹

1.2.4 Ruthenium based anticancer drug candidates

KP1019 and NAMI-A: Ruthenium complexes in clinical testing

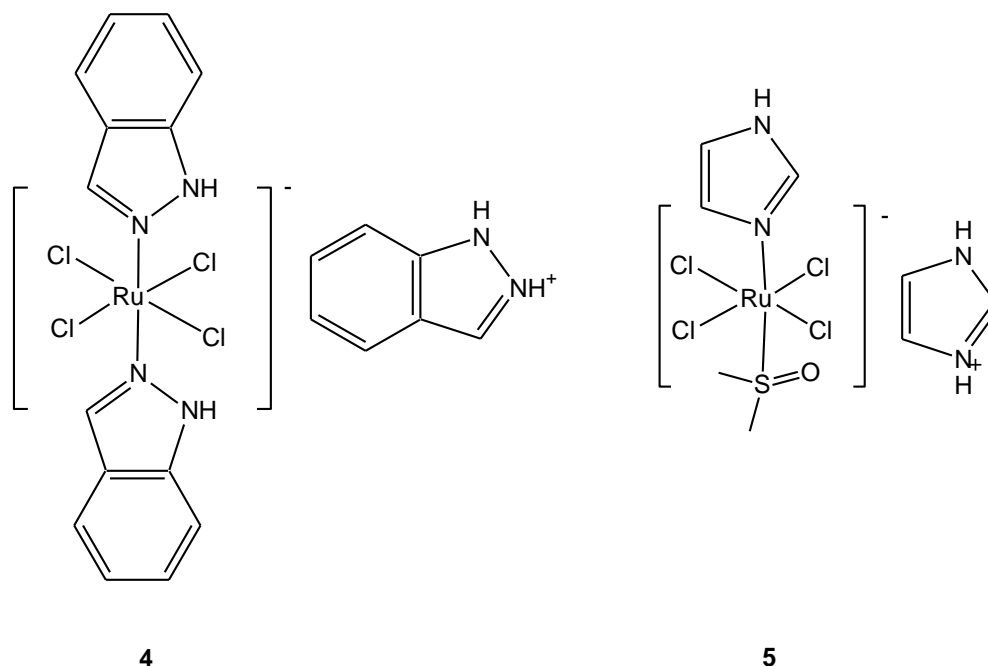


Figure 6. Ruthenium(III) complexes in clinical testing. **4:** KP1019, **5:** NAMI-A.

Two Ru(III) complexes, namely KP1019 (**4**) and NAMI-A (**5**), have been evaluated in clinical trials so far. Both complexes show low general toxicity and negligible side effects.⁴⁰

KP1019 and its sodium salt KP1339 show both higher antitumor activity than cisplatin, for example in colorectal carcinomas *in vivo* and explanted human tumors *in vitro*.⁴¹ Still, the mechanism of action is not fully understood, at least at the molecular level,⁴² but it was observed that it often induces apoptosis in the cancer cell.⁴³ Cell uptake is faster for the sodium salt. It is believed that HSA and transferrin play an important role in drug uptake.⁴⁴ Presumably $[trans-RuCl_4(Hind)_2]^-$ acts as a prodrug and is hydrolyzed to $[mer,trans-RuCl_3(H_2O)(Hind)_2]$.⁴²

NAMI-A is active against metastasis, e.g. in the lung, without significantly influencing primary tumor growth⁴⁵ due to its antiangiogenic properties. Angiogenesis (the formation of new blood vessels) has been recognized as a key event in tumor progression and metastasizing process, the inhibition of neo-vessel formation comes is a viable approach in anticancer therapy.

In vitro NAMI-A shows no cytotoxicity up to mM concentrations.⁴⁶ The mode of action of NAMI-A is not fully understood, but its antiangiogenic and anitnvasive properties seem to be associated with the capturing NO produced by endothelial cells.⁴⁷ The control of angiogenesis was shown in the chick allantoic membrane and in the eye cornea model in the rabbit.^{48,49}

In 2013 Büchel *et al.* reported the synthesis of $(\text{H}_2\text{Ind})/\text{Na}[\text{cis/trans-MCl}_4\text{NO}(\text{Hind})]$, where $M = \text{Ru}, \text{Os}$, the IC_{50} values of the ruthenium compounds were significantly lower than those of the osmium analogues.⁵⁰

RAPTA- type complexes

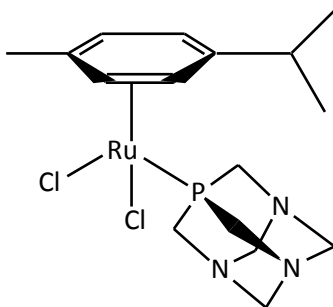


Figure 7. $[\text{Ru}(\eta^6\text{-pcymol})\text{Cl}_2(\text{pta})]$ (pta = 1,3,5-triaza-7-phosphatricyclo-[3.3.1.1]decane), termed RAPTA-T.

RAPTA compounds, defined by a η^6 -arene and a PTA ligand coordinated to Ru, show very similar *in vivo* and *in vitro* effects compared to NAMI-A.⁵¹ Just like in the case of NAMI-A its mode of action is not yet understood. It is suggested, that it is involved in intra- and extra cellular processes and clearly differs from classical Pt-compounds. It

was observed that hydrolysis of the Cl⁻ ligands has no significant influence on cytotoxicity. Moreover it was established that protein binding, e.g. to HSA, is preferred over DNA binding.⁵¹

1.3 NO - a noninnocent ligand

Until 1970, when the physiological effects of NO were reported first by Ferid Murad,⁵² nitric oxide was considered as harmful substance and toxic gas. It is a carcinogen, harmful to the ozone layer and a precursor to acid rain.⁵³ The harmful effects of NO are partly due to its properties as a free radical and thus it can cause oxidative damage. Additionally NO is able to bind irreversibly to metal centers in biological molecules like CO or CN⁻ and therefore is poisonous.⁵⁴

On the other hand many beneficial physiological effects are known nowadays:

- It decreases blood pressure by relaxing smooth muscles in endothelial cells.
- It is generated by Macrophage cells for self-defense against pathogens and microorganisms
- NO controls the release of several neurotransmitters in neuronal cells
- It plays a role in synaptic plasticity, memory function, and neuroendocrine secretion.⁵⁵

In the body a family of nitric oxide synthases (NOS) produces NO from L-arginine.

The affinity of Ru(III)/(II) to NO is well documented in the literature.⁵⁶ NAMI-A scavenges NO and [Ru(edta)(H₂O)]⁻ was designed to bind NO, if the immune system overproduces it due to a septic shock.⁵⁷

In contrast Ru-NO complexes were designed to achieve a controlled release of NO. Several medical applications are considered for such compounds, e.g. the decrease of blood pressure by vasodilation.⁵⁸

Ru-NO complexes are also interesting as anti-tumor prodrugs. Possibilities to release NO within tumor cells^{59,60} are explored as it was found that uncontrolled NO release

leads to DNA cleavage and apoptosis. This was proven in pancreatic cells, leukemia cells and neuronal cells.^{61,62,63}

NO release can be triggered by one electron reduction or by photolysis (highly relevant for photodynamic therapies).⁵⁹

Logically it depends on the lability of the Ru-NO bond, how easily NO is released. Linearly bonded NO is a weak σ donor but a strong π acceptor⁶⁴ and therefore another π acceptor in *trans* position facilitates NO release due to competition for electron density, a strong σ donor, however, strengthens the Ru-NO bond.

Formally the $\{\text{RuNO}\}^6$ entity can be considered as $\{\text{Ru}^{\text{II}}(\text{NO}^+)\}^6$ with a strong π back donation from Ru(II) to NO or as $\{\text{Ru}^{\text{III}}(\text{NO}^0)\}^6$. The second resonance structure fits better to physical and spectroscopic properties of the entity.⁶⁵

1.4 α - Amino acids – The smallest biological ligands

Overview on the 20 proteinogenic amino acids

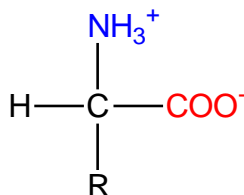


Figure 8. The zwitterionic form of an L- α -amino acid.

Figure 8 shows the general structure of an α -amino acid. Only the L enantiomers are used by nature. At physiological pH (7.4) they are predominantly zwitterions. The pH where the overall charge is zero is called isoelectric point.

There are 20 proteinogenic α -amino acids, which differ in their side chains (represented by “R” in Figure 8). They are indicated by trivial names, a three letter and a one letter code.⁶⁶

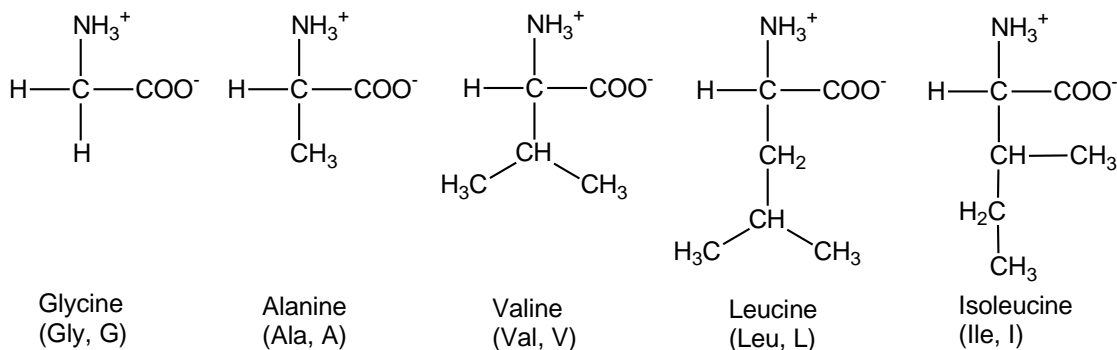


Figure 9. The aliphatic amino acids.

There are five amino acids with aliphatic side chains, namely Glycine, the simplest and only achiral amino acid, with just a hydrogen atom as side chain, alanine, valine, leucine and isoleucine. The larger the side chain gets, the more hydrophobic the amino acid becomes. Isoleucine contains a second center of asymmetry with L configuration.⁶⁶

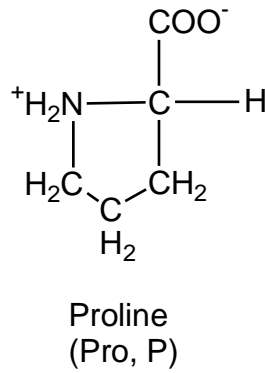


Figure 8. L-Proline, the only cyclic amino acid used by nature.

Proline has also an aliphatic side chain, which is bound to the C and the N terminus and thereby differs from the other proteinogenic amino acids. Proline is well soluble in water and often found in the bends of folded protein chains.

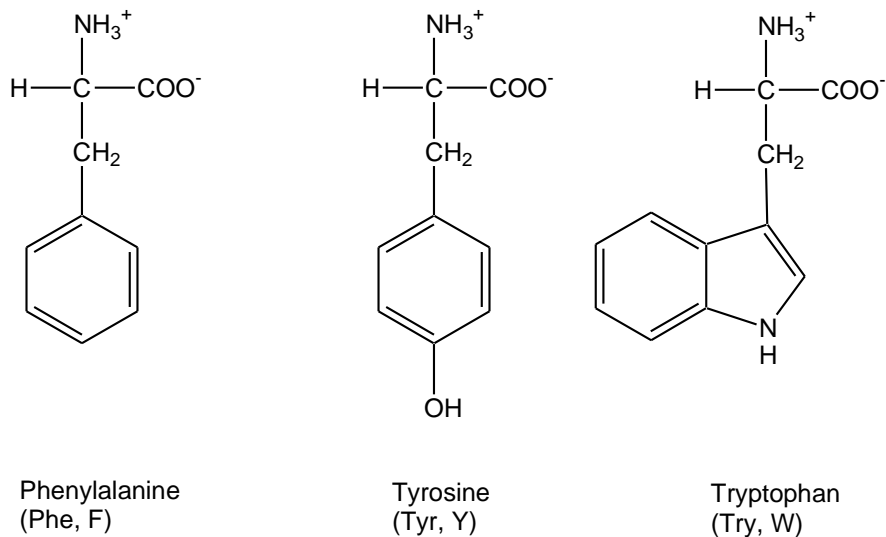


Figure 7. The aromatic amino acids Phenylalanine, Tyrosine and Tryptophan.

Phenylalanine and tryptophan are very hydrophobic; tyrosine is more polar and more reactive due to its hydroxyl group. The aromatic system allows interactions with other π systems and electron transfer.

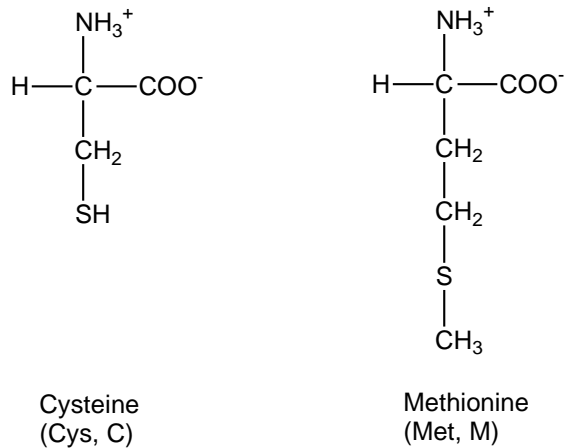


Figure 9. The sulfur containing amino acids Phenylalanine, Tyrosine and Tryptophan.

The sulfur containing amino acids cysteine and methionine play a crucial role in the tertiary structure formation via disulfide links.

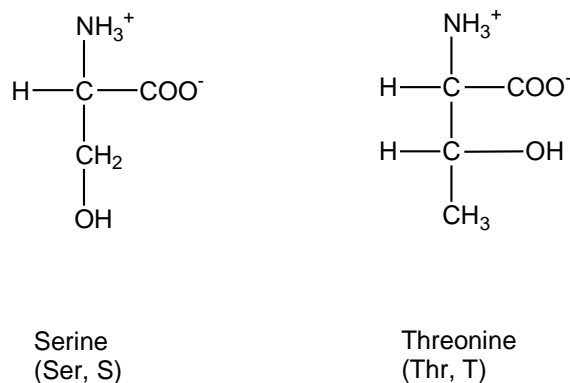


Figure 10. The amino acids Serine and Threonine, which contain aliphatic hydroxyl groups.

Due to their hydroxyl groups serine and threonine are much more hydrophilic and reactive than the aliphatic amino acids. Like isoleucine threonine has two asymmetric centers, both S configured.⁶⁶

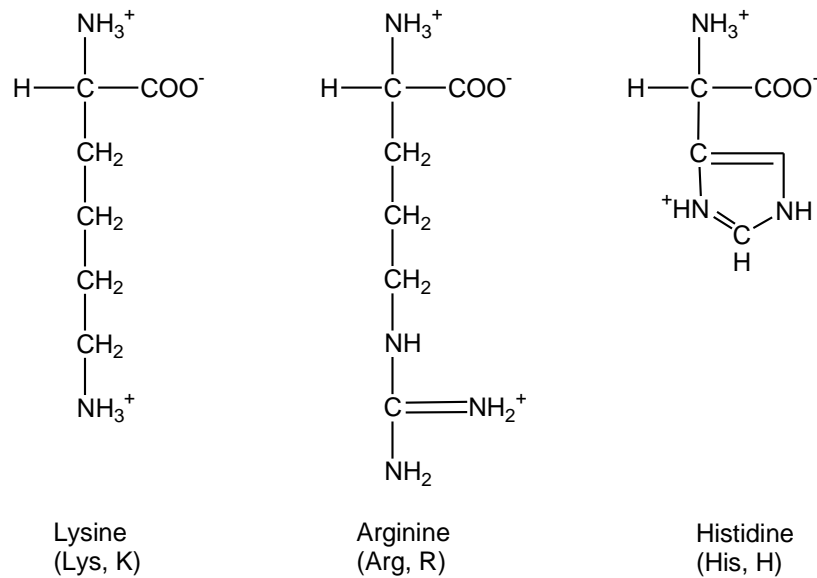


Figure 10. The basic amino acids lysine, arginine and histidine.

Due to the polar side chains, the basic amino acids are highly hydrophilic. The side chains of lysine and arginine are positively charged at neutral pH. Histidine can easily switch between positively and uncharged side chain and is therefore often located at the active site of enzymes to catalyze the formation or dissociation of bonds.⁶⁶

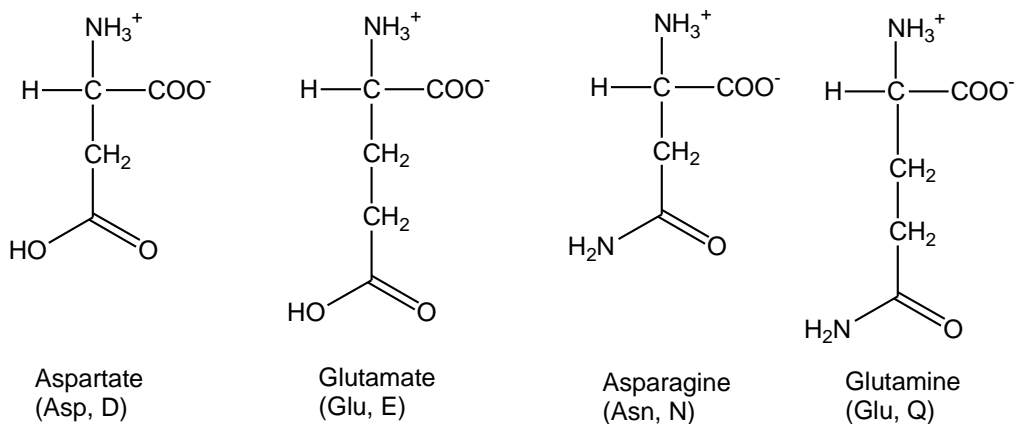


Figure 11. The acidic amino acids aspartate and glutamate and their amides asparagine and glutamine.

Two amino acids with acid groups in the side chain belong to the set of 20 amino acids. As the names, aspartate and glutamate, imply, their side chains are nearly always

negatively charged at physiological pH. Their amide derivatives asparagine and glutamine are usually uncharged.⁶⁶

The amino acids isoleucine, leucine, lysine, methionine, phenylalanine, threonine, tryptophan are essential, which means that they must be supplied with food.

1.5 Ruthenium complexes with amino acids

Amino acids are known to bind metal ions as bidentate ligands. As N,O-donors they form five membered chelate rings. The carboxyl group is deprotonated, the amine is a neutral ligand.

Amino acids are the basic units of proteins and of crucial importance for life. Therefore the behavior of (potential) anticancer drugs towards them is highly interesting. It can provide information about the species that may be formed in cellular media, the blood, where free amino acids occur, as well as possible metabolites in the body. A $[(Pt(L-Met)_2)]$ species was isolated from the urine of cancer patients treated with cisplatin. This is one of the few known metabolites of the drug.⁶⁷

Ruthenium complexes with amino acids are not only relevant in anticancer research. Due to the chirality of all amino acids except glycine Ru-AA complexes are optically active. Therefore applications as enantioselective oxidants/reductants or catalysts, enantioselective quenchers of luminescence and DNA recognition are possible. Especially, bis(diimine)-type ruthenium(II) complexes with chiral ligands were studied. These complexes are, in general, fairly stable and reliable synthesis routes are known.⁶⁸

Several ruthenium(II) complexes with amino acids are used as catalysts for the enantioselective epoxidation of olefins.⁶⁹

In particular, Schiff base complexes of the type $[Ru(II)(L)(PPh_3)(H_2O)_2]^+$ where L = salicylaldehyde derivative or an L amino acids, e.g. valine, serine, cysteine or aspartate catalyze the asymmetric epoxidation of styrene.⁷⁰

Ruthenium(II) polypyridyl complexes show interesting photophysical and photochemical properties. They exhibit intense MLCT luminescence, excited state redox properties and the ability to bind to the DNA. Therefore they attracted research interest in the last decades. A series of $[\text{Ru}(\kappa^3\text{-tptz})(\text{AA})(\text{PPh}_3)]\text{BF}_4$ complexes was prepared by Kumar *et al.* These complexes behave as good precursors and act as metallo-ligands in the synthesis of homo-/hetero bimetallic complexes. Furthermore they inhibit topoisomerase II and heme polymerase.⁷¹

Another example is the $[\text{Ru(II/III)}(\text{bcmaa})\text{R}(\text{bpy})]$ complex illustrated in Figure 12 that can be used as a redox partner for electron transfer proteins as azurin or plastocyanin to investigate the electron-transfer site. It was observed that the electron transfer from az-Cu(I) to one of the R enantiomers of $[\text{Ru(III)}(\text{L})(\text{byp})]$ is 1.3 –1.7 times faster than to an S enantiomer.

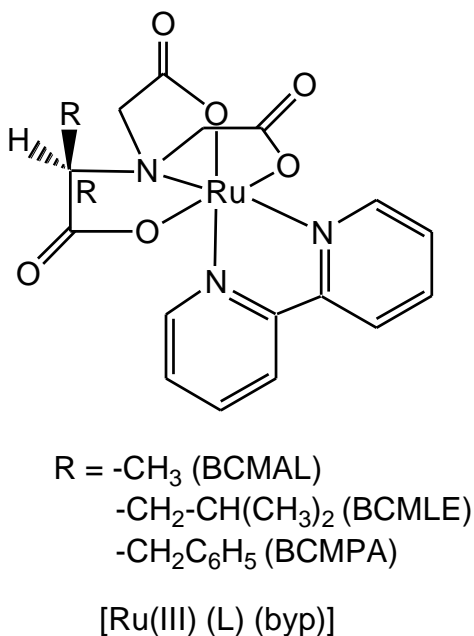


Figure 12. $[\text{Ru(III)}(\text{L})(\text{byp})]$ in with the amino acids alanine, leucine and phenylalanine in R configuration.⁷²

Ruthenium–NO complexes with amino acids

In 1979, the synthesis of $\text{K}[\text{Ru}(\text{Gly})(\text{OH})_3\text{NO}]$ was published by Ishiyama and Matsumura. The complex was characterized by elemental analysis, IR and UV–vis spectroscopy.⁷³

In 1980, the synthesis of $\text{K}[\text{Ru}(\text{L-Ala})(\text{OH})_3\text{NO}]$ followed. These complexes were prepared to study the behavior of the $\{\text{RuNO}\}^6$ entity in marine environment, a most crucial point in the assessment of the impact of radioactive transition metals on sediments and organism.⁷⁴

In 2009 the synthesis and characterization of $[\text{Ru}(\text{Cl})_2\text{NO}(\text{L-His})]$ was reported.⁷⁵

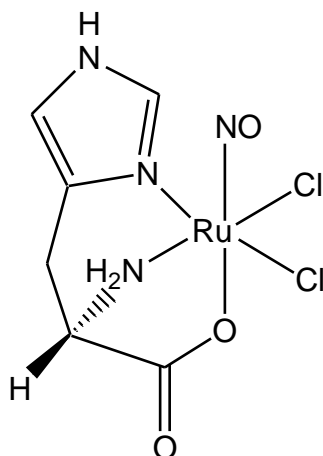


Figure 13. $[\text{Ru}(\text{L-His})(\text{Cl})_2\text{NO}]$ published by Zangl *et al.* in 2009

Furthermore synthesis and characterization of $(\text{C}_2\text{H}_2)\text{N}[\text{RuCl}_3\text{NO}(\text{pyca})]$ were published in 2003.⁷⁶

-
- ¹ WHO. <http://www.who.int/cancer/en/index.html>. (accessed May 8, 2013).
 - ² Statistik Austria.
http://www.statistik.at/web_de/statistiken/gesundheit/krebserkrankungen. (accessed May 8, 2013)
 - ³ GLOBOCAN 2008 (IARC) *Section of Cancer Information (8/5/2013)*.
<http://globocan.iarc.fr/factsheets/populations/factsheet.asp?uno=900>. (accessed May 8, 2013).
 - ⁴ Weinberg, R. A. *The biology of cancer*. Garland Science: New York, **2007**, 26–28
 - ⁵ Alberts, B.; Johnson A.; Lewis, J.; Raff, M.; Roberts, K.; Walter, P. *Molecular Biology of the cell* Garland Science: New York, **2008**, 1206–1265
 - ⁶ Goodsell, D.S. *The Oncologist* **1999**, 4 (3), 4–263.
 - ⁷ Pardee, A. B.; Stein, G. S., *The biology and treatment of cancer: Understanding cancer*. Wiley-Blackwell: Hoboken, New Jersey, **2009**, 10–21
 - ⁸ Price, P.; Sikora, K.; Illidge, T. *Treatment of cancer*. Hodder Arnold: London, **2008**, 75–112.
 - ⁹ Lippert, B. *Cisplatin*. Helvetica Chimica Acta: Zürich, **1999**, 3–7.
 - ¹⁰ Lippert, B. *Cisplatin*. Helvetica Chimica Acta: Zürich, **1999**, 31–73.
 - ¹¹ Loehrer, P.J.; Einhorn L. H. *Ann. Intern. Med.* **1984**, 100, 704.
 - ¹² Harrap, K.R. *Cancer Treat. Rev.* **1985**, 12, 21.
 - ¹³ Calvert, A.H.; Newell, D.R.; Gumbrell, L.A.; O'Reilly, S.; Burnell, M.; Boxall, F.E.; Siddik, Z.H.; Judson, I.R.; Gore, M.E.; Wiltshaw, E. *J. Clin. Oncol.* **1989**, 7, 1748.
 - ¹⁴ Alberts, D.S.; Green, S.; Hannigan, E.V.; O'Tool, R.; Stock-Novack, D.; Anderson, P.; Surwite, A.; Malvly, V.K.; Nahas, W.A.; Jolles, C.J. *J. Clin. Oncol.* **1992**, 10, 706.
 - ¹⁵ Extra, J.M.; Espic, M.; Calvo, F.; Ferme, C.; Mignot, L.; Marty, M. *Cancer Chemother. Pharmacol.* **1990**, 25, 299.
 - ¹⁶ Tashiro, R.; Kawada, Y.; Sakuri, Y.; Kidani, Y. *Biomed. Pharmacother.* **1989**, 43, 251.
 - ¹⁷ Mathe, G.; Kidani, Y.; Sekiguchi, M.; Eriguchi, M.; Fredj, G.; Peytavin, G.; Misset, L.J.; Brienza, S.; de Vassals, F.; Chenu, E. *Biomed. Pharmacother.* **1989**, 43, 237.

-
- ¹⁸ Jennerwein, M.M.; Eastman, A.; Khokhar, A. *Chem. Biol. Interact.* **1989**, *70*, 39.
- ¹⁹ Saris, C.P.; van der Vaart, P.J.M.; Rietbroek, R.; Blommaert, F.A. *Carcinogenesis*, **1996**, *17*, 2763.
- ²⁰ Kraker, A.J.; Moore, C.W. *Cancer Res.* **1988**, *48*, 9.
- ²¹ Becouarn Y.; Ychou M.; Ducreux M. *et al. J Clin Oncol* **1998**, *16* (8), 2739–44.
- ²² Grubbs R.H. *Handbook of Metathesis*. Wiley-VCH: Weinheim. **2003**, .
- ²³ M. J. Clarke, *Coord. Chem. Rev.*, **2003**, *236*, 210.
- ²⁴ Hartmann, M.; Kepler, B.K. *Comm. Inorg. Chem.*, **1995**, *16*, 339.
- ²⁵ Gray, H.B.; Winkler, J.R. *Ann. Rev. Biochem.*, **1996**, *65*, 37.
- ²⁶ Ditrach, C.; Scheulen, M.E.; Jaehde, U.; Kynast, B.; Gneist, M.; Richly, H.; Schaad, S.; Arion, V.B.; Kepler, B.K. *Proc. Am. Assoc. Cancer Res.*, **2005**, *46*, 472.
- ²⁷ Kuehn, C.G.; Taube, H. *J. Am. Chem. Soc.*, **1976**, *98*, 689.
- ²⁸ Clarke, M.J.; Dowling, M.G. *Inorg. Chem.*, **1981**, *20*, 3506.
- ²⁹ Palmer, B.D.; Wilson, W.R.; Pullen, S.M. *J. Med. Chem.*, **1990**, *33*, 112.
- ³⁰ Wike-Hooley, J.L.; Haveman, J.; Reinhold, H.S. *Radiother. Oncol.*, **1984**, *2*, 343.
- ³¹ Marchant, J.A.; Matsubara, T.; Ford, P.C. *Inorg. Chem.*, **1977**, *16*, 2160.
- ³² Miklavcic, D.; Sersa, G.; Novakovic, S. *J. Bioelect.*, **1990**, *9*, 133.
- ³³ Neidle, S. *NATURE CHEMISTRY*, **2012**, *4*, 594.
- ³⁴ Clarke, M.J.; Bitler, S.; Rennert, D.; Buchbinder, M.; Kelman, A.D. *J. Inorg. Biochem.*, **1980**, *12*, 79.
- ³⁵ Stanbury, D.M.; Haas, O.; Taube, H.; *Inorg. Chem.*, **1980**, *19*, 518.
- ³⁶ Messori, L.; Vilchez, F.G.; Vilaplana, R.; Piccioli, F.; Alessio, E.; Kepler, B. *Met. Based Drugs*, **2000**, *7*, 335.
- ³⁷ Dömötör, O.; Hartinger, C.; Bytzek, A.; Kiss, T.; Kepler, B.; Enyedy, E. *J Biol Inorg Chem.*, **2013**, *18*, 9–17
- ³⁸ E.; Garratt, R.W.; Richard, G. *Biochemistry*, **1988**, *27*, 5804.
- ³⁹ Som, P.; Oster, Z.H.; Matsui, K.; Gugliemi, G.; Persson, B.; Pellettieri, M.L.; Srivastava, S.C.; Richards, P.; Atkins, H.L.; Brill, A.B. *Eur. J. Nucl. Med.*, **1983**, *8*, 491.

-
- ⁴⁰ Jakupec, M. A.; Galanski, M.; Arion, V. B.; Hartinger, C. G.; Keppler, B. K. *Dalton Trans.* **2008**, 2, 183-194.
- ⁴¹ Hartinger, C. G.; Zorbas-Seifried, S.; Jakupec, M. A.; Kynast, B.; Zorbas, H.; Keppler, B. K. *Inorg. Biochem.*, **2006**, 100, 891–904.
- ⁴² Cebrián-Losantos, B.; Reisner, E.; Kowol, C.; Roller, A.; Shova, S.; Arion, V.; Keppler, B. *Inorg. Chem.* **2008**, 47, 6513–6523.
- ⁴³ Heffeter, P.; Böck, K.; Atil, B.; Reza Hoda, M.; Körner, W.; Bartel, C.; Jungwirth, U.; Keppler, B.; Micksche, M.; Berger, W.; Koellensperger, J. *Biol. Inorg. Chem.*, **2010**, 15, 737–748.
- ⁴⁴ Jakupec, M. A.; Reisner, E.; Eichinger, A.; Pongratz, M.; Arion, V. B.; Galanski, M.; Hartinger, C. G.; Keppler, B. K. *J. Med. Chem.*, **2005**, 48, 2831–2837.
- ⁴⁵ Sava G.; Capozzi I.; Clerici K.; Gagliardi R.; Alessio E.; Mestroni G. *Clin. Exp. Met.*, **1998**, 16, 371.
- ⁴⁶ Pacor S.; Vadori M.; Vita F.; Bacac M.; Soranzo MR.; Zabucchi G.; Sava G. *Anticancer Res*, **2001**, 21, 2523.
- ⁴⁷ Serli, B.; Zangrado, E.; Iengo, E.; Mestroni, G.; Yellowlees, L.; Alessio, E. *Inorg. Chem.* **2002**, 41, 4033–4043
- ⁴⁸ Vacca, A.; Bruno, M.; Boccarelli, A.; Coluccia, M.; Ribatti, D.; Bergamo, A.; Garbisa, S.; Sartor, L.; Sava, G. *Brit. J. Cancer* **2002**, 86, 993–998.
- ⁴⁹ Morbidelli, L.; Donnini, S.; Filippo, S.; Messori, L.; Piccioli, F.; Orioli, P.; Sava, G.; Ziche, M. *Brit. J. Cancer* **2003**, 88, 1484–1491.
- ⁵⁰ Büchel, G.; Gavrilluta, A.; Novak, M.; Meier, S.; Jakupec, M.; Cuzan, O.; Turta, C.; Tommasino, J.; Jeanneau, E.; Novitchi, G.; Luneau, D.; Arion, V. *Inorg. Chem.*, **2013**, 52, 6273–6285
- ⁵¹ Ang W.H. et al *Journal of Organometallic Chemistry*, **2011**, 696, 989–998.
- ⁵² <http://www.britannica.com/EBchecked/topic/397831/Ferid-Murad>, (accessed June 3, 2013).
- ⁵³ Culotta, E.; Koshland, Jr., D.E. *Science* **1992**, 258, 1862–1864.
- ⁵⁴ McCleverty, J.A. *Chem. Rev.* **2004**, 104, 403–418.
- ⁵⁵ Silverman, R.B. *Acc. Chem. Res.* **2009**, 42, 439–445.

-
- ⁵⁶ Serli, B.; Zangrado, E.; Gianferrara, T.; Yellowlees, L.; Alessio, E. *Coord. Chem. Rev.* **2003**, *245*, 73–83.
- ⁵⁷ (a) Fricker, S.P.; Slade, E.; Powell, N.A.; Vaughn, O.J.; Henderson, G.; Murrer, S.A.; Megson, I.C.; Bisland, S.K.; Fitney, F.W. *Br. J. Pharmacol.* **1997**, *122*, 1441–1449.
- (b)
Davies, N.; Wilson, M.T.; Slade, E.; Fricker, S.P.; Murrer, B.A.; Powell, N.A.; Henderson, G.R. *J. Chem. Soc., Chem. Commun.* **1997**, 47–48.
- ⁵⁸ Lang, D.R.; Davis, J.A.; Lopes, L.G.F.; Ferro, A.A.; Vasconcellos, L.C.G.; Franco, D.W.; Tfouni, E.; Wieraszkowski, A.; Clarke, M.J. *Inorg. Chem.* **2000**, *39*, 2294–2300.
- ⁵⁹ Slocik, J.M.; Shepherd, R.E. *Inorg. Chim. Acta* **2000**, *311*, 80–94.
- ⁶⁰ Slocik, J.M.; Ward, M.S.; Somayajula, K.V.; Shepherd, R.E. *Transition Met. Chem.* **2001**, *26*, 351–364.
- ⁶¹ Kaneto, H.; Fujii, J.; Suzuki, K.; Matsuoka, T.; Nakamura, M.; Tasumi, H.; Kamada, T.; Taniguchi, N. *Diabetes*, **1995**, *44*, 733–738.
- ⁶² Ho, Y.S.; Lec, H.H.; Mori, T.C.; Wong, Y.J.; Lin, J.K. *Mol. Carcinogenesis* **1997**, *19*, 101–113.
- ⁶³ (a) Messmer, U.K.; Reed, J.C.; Bruene, B. *J. Biol. Chem.* **1996**, *271*, 20192–20197.
- (b) Bruene, B.; Messmer, U.K.; Sandau, K. *Toxicol. Lett.* **1995**, *82/83*, 233–237.
- ⁶⁴ Toshiyuki H.; Takao O.; Hirota N.; Keiji M. *Inorg. Chem.*, **2003**, *42*, 6575–6576.
- ⁶⁵ Bučinský, L.; Büchel, G.; Ponec, R.; Raptá, P.; Breza, M.; Kožíšek, J.; Gall, M.; Biskupič, S.; Fronc, M.; Schiessl, K.; Cuzan, O.; Prodius, D.; Turta, C.; Shova, S.; Zając, D.; Arion, V. *Eur. J. Inorg. Chem.*, **2013**, 2505–1519.
- ⁶⁶ Stryer, L. *Biochemistry* W.H. Freeman & Company: New York, **1995**, 19–25.
- ⁶⁷ Prestaiko, A. W., Carter, S. K. *Academic Press*: New York, **1980**; 285–304.
- ⁶⁸ Tamura, M.; Yamagishi, M.; Kawamoto, T.; Igashira-Kamiyama, A.; Tsuge, K.; Konno T. *Inorg. Chem.* **2009**, *48*, 8998–9004.
- ⁶⁹ Kureshy, R.I.; Khan, N.; Abdi, S.H.; Patel, S.T.; Iyer P. *Journal of Molecular Catalysis*, **1999**, 163–173.

-
- ⁷⁰ Rukhsana, K.; Khan, N.; Abdi, S.; Bhatt, K. *Tetrahedron: Asymmetry*, **1993**, 7, 1693—1701.
- ⁷¹ Kumar, P.; Kumar, S.A.; Kumar, J.S.; Pandey D.S. *J. Organomet. Chem.*, **2009**, 3570–3579.
- ⁷² H. Kumita et al. *Inorg. Chem. Communications*, **2000**, 3, 185–187.
- ⁷³ Ishiyama T.; Matsumura T. *Bull. Chem. Soc. Jpn.*, **1979**, 52, 619—620.
- ⁷⁴ Ishiyama T.; Matsumura T. *Annual Report of the Radiation Center of Osaka Prefecture*, **1980**, 21, 7–9.
- ⁷⁵ Zangl, A.; Klufers, P.; Schaniel D.; Woike, T. *Dalton Trans.*, **2009**, 1034–1045.
- ⁷⁶ Hirano, T.; Oi, T.; Nagao, H.; Morokuma, K., *Inorg. Chem.*, **2003**, 42, 6575—6583.

Abstract

Amino acids are the most important biological ligands with low molecular weight in the human body. Nevertheless very little is known about the reactivity of amino acids towards ruthenium-nitrosyl complexes, which are interesting anti-tumor compounds. We intended to close that gap and decided to prepare a series of ruthenium-nitrosyl complexes with amino acids of the general formula $\text{Bu}_4\text{N}[\text{RuCl}_3\text{NO}(\text{L})]$, where L = L-Ala, L-Val, Gly, L-Ser, L-Thr, L-Tyr, L-Pro, D-Pro. The compounds were characterized by elemental analysis, ESI MS, ^1H NMR, UV-vis, ATR IR spectroscopy, cyclic voltammetry and X-ray crystallography. Furthermore cell culture experiments in three human cancer cell lines were performed and IC_{50} values were determined.

Introduction

Since the discovery of cisplatin, platinum(II) compounds have become an integral part of anticancer chemotherapy. Despite remarkable cure rates for some types of cancer, the search for metal-based drugs continues because of severe side effects of approved platinum compounds and the resistance of some tumor types. Ruthenium and osmium(II)/(III) compounds are promising anti-cancer agents, although their mode of action remains unknown at least at the molecular level. The anti-angiogenic and anti-invasive properties of NAMI-A were reported to be connected at least in part to NO capturing. In addition, nitric oxide is an interesting ligand for potential anticancer agents, and is a typical example of a non-innocent ligand.¹

As a small signal molecule it is involved in blood pressure regulation, inflammatory response and in necrosis.² The affinity of Ru(II)/(III) to NO is well documented in the literature.³ Ruthenium-nitrosyl complexes were also designed to achieve a controlled release of NO. Several medical applications are considered for such compounds, e.g. the decrease of blood pressure by vasodilation.⁴ It was found that uncontrolled NO release leads to DNA cleavage and apoptosis. This was proven in pancreatic cells, leukemia cells and neuronal cells^{5,6,7}. Therefore ruthenium-nitrosyl complexes, which could release NO within tumor cells are worthy to be investigated.^{8,9}

NO release can be triggered by one-electron reduction or by photolysis (highly relevant for photodynamic therapies).⁵⁹ It depends on the lability of the Ru-NO bond, how easily NO is released. NO can bind to metal ions linearly as NO or NO⁺ or as a bent NO⁻ ligand. Linearly bound NO and/or NO⁺, show structural *trans* effects (STE), depending on the *trans* ligand.¹⁰ It is a weak σ donor but a strong π acceptor¹¹ and therefore another π acceptor in *trans* position facilitates NO release due to competition for electron density. A strong σ donor, however, strengthens the Ru-NO bond. Formally the {RuNO}⁶ entity can be considered as {Ru^{II}(NO⁺)⁶ with a strong π back donation from Ru(II) to NO or as {Ru^{III}(NO⁰)⁶. The second resonance structure fits better to physical and spectroscopic properties of the entity.¹²

Amino acids are the basic units of proteins and of crucial importance for life. Therefore the study of the behavior of (potential) anticancer drugs towards them is of great importance. It can provide information about the species which may be formed in cellular media or in the blood, where free amino acids occur, as well as about possible metabolites in the body. A [(Pt(L-Met)₂)] species was isolated from the urine of cancer patients treated with cisplatin. This is one of the few known metabolites of the drug.¹³

Amino acids are known to coordinate to metal ions as bidentate ligands. As N,O-donors they form five-membered chelate rings. The carboxyl group is deprotonated, the amine is a neutral ligand.

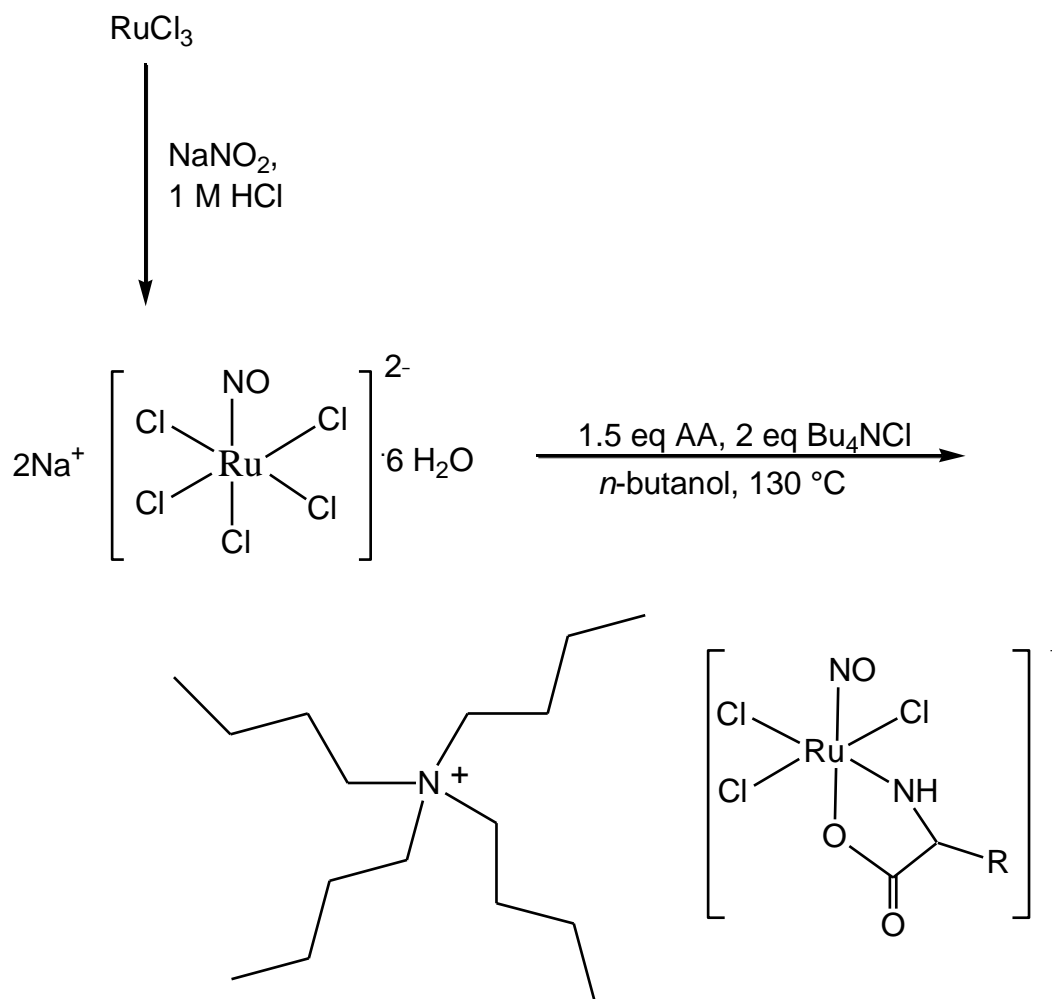
Only a few ruthenium-nitrosyl complexes with amino acids and related ligands have been reported in the literature, e.g. K[Ru(Gly)(OH)₃NO]¹⁴, K[Ru(L-Ala)(OH)₃NO]¹⁵, [Ru(Cl)₂NO(L-His)]¹⁶ and (C₂H₅)₄N[RuCl₃NO(pyca)].¹⁷

However, for none of the ruthenium-nitrosyl complexes published so far the cytotoxicity was tested. We prepared a series of ruthenium-nitrosyl complexes with amino acids, Bu₄N[RuCl₃NO(L)] (L = L-Ala, L-Val, Gly, L-Ser, L-Thr, L-Tyr, L-Pro, D-Pro). The compounds have been characterized by elemental analysis, ESI MS, ¹H NMR, UV-vis, ATR IR spectroscopy, cyclic voltammetry and X-ray crystallography. The antiproliferative activity of these ruthenium complexes has been assayed in three human cancer cell lines, namely A549 (nonsmall lung carcinoma, CH1 (ovarian carcinoma) and SW480 (colon adenocarcinoma).

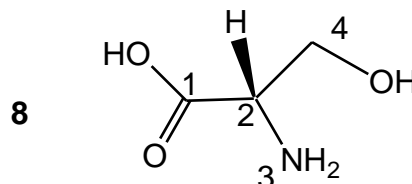
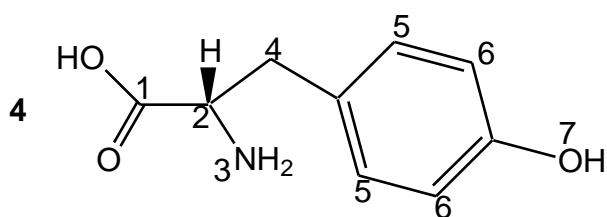
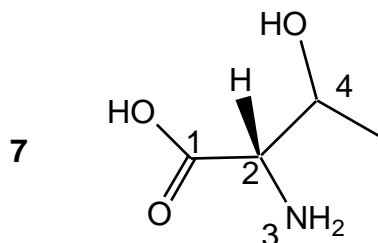
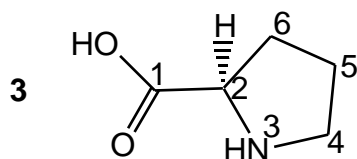
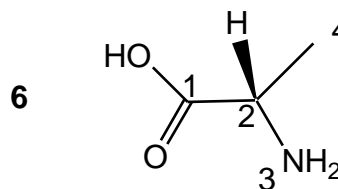
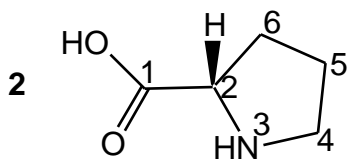
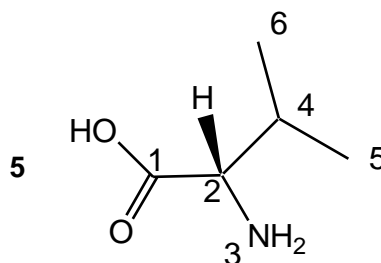
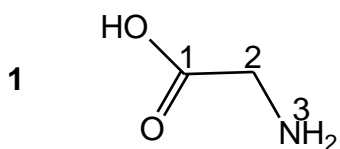
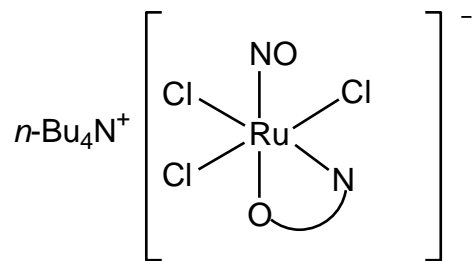
2 Experimental Sections

2.1 Synthesis and characterization of ruthenium-nitrosyl complexes with amino acids

Synthetic Scheme



Numbering scheme



Materials and methods

Materials. The starting compounds $\text{Na}_2[\text{RuCl}_5\text{NO}] \cdot 6\text{H}_2\text{O}$ and $(\text{Bu}_4\text{N})_2[\text{RuCl}_5\text{NO}]$ were synthesized as previously reported in the literature.^{18,19} $\text{RuCl}_3 \cdot \text{H}_2\text{O}$ was purchased from Johnson Matthey, Sodium nitrite (+97%), tetrabutylammonium chloride (+97%), L-threonine, L-alanine and glycine (99%) were from Sigma-Aldrich. L-Serine was from Serva, D-proline (99%) and L-proline (99%) were from Alfa Aesar and L-tyrosine (99%) was from Fulka. All chemicals were used without further purification.

$(\text{Bu}_4\text{N})[\text{RuCl}_3\text{NO}(\text{Gly})]$ (1). A mixture of $\text{Na}_2[\text{RuCl}_5\text{NO}] \cdot 6\text{H}_2\text{O}$ (400 mg, 0.87 mmol), Bu_4NCl (362 mg, 1.31 mmol) and glycine (121 mg, 1.61 mmol) was refluxed in *n*-butanol (10 mL) for 1.5 h. The solution was allowed to cool to room temperature. The separated salt was filtered. The solution was transferred into a beaker. Dark red crystals formed after several days were filtered off and washed with water/ethanol 1 : 3 (4 mL), diethyl ether (4 mL) and dried *in vacuo*. Yield: 75 mg, 13%. Anal. Calcd for $\text{C}_{18}\text{H}_{40}\text{Cl}_3\text{N}_3\text{O}_3\text{Ru}$ ($M_r = 553.96$ g/mol): C, 39.03; H, 7.28; N, 7.59. Found: C, 38.77; H, 6.96; N, 7.43. ESI MS in MeOH (negative): m/z 312 $[\text{RuCl}_3\text{NO}(\text{Gly})]^-$, 276 $[\text{RuCl}_2\text{NO}(\text{Gly})\text{-HCl}]^-$, 240 $[\text{RuClNO}(\text{Gly})\text{-2HCl}]^-$. IR, cm^{-1} : 886, 1160, 1301, 1490, 1669, 1862, 2955, 3744 and 3837. UV-vis (buffer), λ_{max} , nm (ϵ , $\text{M}^{-1}\text{cm}^{-1}$): 279 (1790), 453 (104). ^1H NMR (500.32 MHz, d_6 -DMSO): δ 0.95 (t, 12H_D, $J = 7.5$ Hz), 1.32 (sxt, 8H_C, $J = 7.3$ Hz), 1.58 (qui, 8H_B, $J = 7.8$ Hz), 3.17 (t, 8H_A, $J = 8.2$ Hz), 5.89 (s, 2H, H₃) ppm.

$(\text{Bu}_4\text{N})[\text{RuCl}_3\text{NO}(\text{L-Pro})]$ (2). A mixture of $(\text{Bu}_4\text{N})_2[\text{RuCl}_5\text{NO}]$ (350 mg, 0.44 mmol) and L-proline (76 mg, 0.66 mmol) was refluxed in *n*-butanol (6 mL) for 3.5 h. The solvent was removed under reduced pressure. The remaining oil was dissolved in water (5 mL). The solution was transferred into a beaker and allowed to stand at room temperature. Orange crystals formed were filtered off and a second fraction was collected after 24 h. The product was washed with water/ethanol 1 : 1, diethyl ether and dried *in vacuo*. Yield: 94 mg, 36%. Anal. Calcd for $\text{C}_{21}\text{H}_{43}\text{Cl}_3\text{N}_3\text{O}_3\text{Ru}$ ($M_r = 593.01$ g/mol): C, 42.53; H, 7.31; N, 7.09. Found: C, 42.48; H, 7.37; N, 6.78. ESI MS in MeOH (negative): m/z 351 $[\text{RuCl}_3\text{NO}(\text{L-Pro})]^-$, 279 $[\text{RuClNO}(\text{L-Pro})\text{-2HCl}]^-$. IR, cm^{-1} : 740, 883, 1353, 1464, 1644,

1647, 1845, 2874 and 2960. UV-vis (buffer), λ_{\max} , nm (ϵ , $M^{-1}cm^{-1}$): 279 (1981), 253 (104). 1H NMR (500.32 MHz, d_6 -DMSO): δ 0.95 (t, 12H_D, J = 7.4 Hz), 1.32 (sxt, 8H_C, J = 7.4 Hz), 1.58 (qui, 8H_B, J = 7.8 Hz), 1.69 (m, 1H, H₅'), 1.85 (m, 2H, H₆', H₅''), 2.05 (m, 1H, H₆''), 2.87 (m, 1H, H₄'), 3.17 (t, 8H_A, J = 8.2 Hz), 3.42 (m, 1H, H₄''), 3.88 (qua, 1H, H₂, J = 7.1 Hz), 7.08 (m, 1H, H₃) ppm.

(Bu₄N)[RuCl₃NO(D-Pro)] (3). A mixture of Na₂[RuCl₅NO]·6H₂O (400 mg, 0.87 mmol), Bu₄NCl (450 mg, 1.62 mmol) and D-proline (148 mg, 1.29 mmol) was refluxed in *n*-propanol (10 mL) for 2 h. The solvent was removed under reduced pressure. Water (7 mL) was added to the residue. The solution was decanted into a beaker and allowed to stand at room temperature. Orange crystals formed were filtered off and a second fraction was collected after 72 h. The product was washed with water/ethanol 50 : 50 (4 mL), diethyl ether (4 mL) and dried *in vacuo*. Yield: 175 mg, 34%. Anal. Calcd for C₂₁H₄₃Cl₃N₃O₃Ru·0.75H₂O (M_r = 606.52 g/mol): C, 41.54; H, 7.33; N, 6.92. Found: C, 41.70; H, 7.68; N, 7.07. ESI MS in MeOH (negative): m/z 351 [RuCl₃NO(D-Pro)]⁻, 279 [RuClNO(D-Pro)-2HCl]⁻. IR, cm^{-1} : 740, 883, 1353, 1464, 1644, 1647, 1845, 2874 and 2960. UV-vis (buffer), λ_{\max} , nm (ϵ , $M^{-1}cm^{-1}$): 279 (1846), 253 (90). 1H NMR (500.32 MHz, d_6 -DMSO): δ 0.95 (t, 12H_D, J = 7.4 Hz), 1.32 (sxt, 8H_C, J = 7.4 Hz), 1.58 (qui, 8H_B, J = 7.8 Hz), 1.69 (m, 1H, H₅'), 1.85 (m, 2H, H₆', H₅''), 2.05 (m, 1H, H₆''), 2.87 (m, 1H, H₄'), 3.17 (t, 8H_A, J = 8.2 Hz), 3.42 (m, 1H, H₄''), 3.88 (qua, 1H, H₂, J = 7.1 Hz), 7.08 (m, 1H, H₃) ppm.

(Bu₄N)[RuCl₃NO(L-Tyr)] (4). A mixture of Na₂[RuCl₅NO]·6H₂O (500 mg, 1.08 mmol), Bu₄NCl (598 mg, 2.16 mmol) and L-tyrosine (294 mg, 1.62 mmol) was refluxed in *n*-butanol (10 mL) for 2 h. The solution was allowed to cool down to room temperature, filtered and transferred into an Erlenmeyer flask. After 12 days dark red crystals formed. were filtered off, washed with water (5 mL), ethanol (5 mL), diethyl ether (5 mL) and dried *in vacuo*. Yield: 274 mg, 38%. Anal. Calcd for C₂₄H₄₄Cl₃N₃O₄Ru (M_r = 660.08 g/mol): C, 45.49; H, 7.02; N, 6.37. Found: C, 45.33; H, 6.85; N, 6.12. ESI MS in MeOH (negative): m/z 419 [RuCl₃NO(L-Tyr)]⁻, 383 [RuCl₂NO(L-Tyr)-HCl]⁻, 347 [RuClNO(L-Tyr)-2HCl]⁻. IR, cm^{-1} : 740, 827, 1183, 1270, 1366, 1466, 1641, 1885, 2962, 3101 and 3169.

UV-vis (buffer), λ_{\max} , nm (ϵ , $M^{-1}cm^{-1}$): 279 (2109), 453 (99). 1H NMR (500.32 MHz, d_6 -DMSO): δ 0.95 (t, 12H_D, $J = 7.4$ Hz), 1.32 (sxt, 8H_C, $J = 7.4$ Hz), 1.58 (qui, 8H_B, $J = 7.8$ Hz), 2.96 (m, 2H, H_{4'}, H_{4''}), 3.17 (t, 8H_A, $J = 8.2$ Hz), 3.75 (m, 1H, H₂), 4.71 (m, 1H H₃), 6.41 (m, 1H, H_{3'}), 6.69 (d, 2H, H₅, $J = 7.4$ Hz), 7.09 (d, 2H, H₅, $J = 8.4$ Hz), 9.22 (s, 1H, H₇) ppm.

(Bu₄N)[RuCl₃NO(L-Val)] (5). A mixture of Na₂[RuCl₅NO]·6H₂O (400 mg, 0.86 mmol), Bu₄NCl (450 mg, 1.62 mmol) and L-valine (151 mg, 1.29 mmol) was refluxed in *n*-butanol (10 mL) for 2 h. The solvent was removed under reduced pressure and the remaining oil was dried *in vacuo*. Water (7 mL) was added. The solution was decanted into a beaker and allowed to stand at room temperature. Seven days later orange crystals formed were filtered off. A second fraction was collected two days later. It was washed with water/ethanol 50 : 50, diethyl ether and dried *in vacuo*. Yield: 179 mg, 35%. Anal. Calcd for C₂₁H₄₆Cl₃N₃O₃Ru·0.5H₂O ($M_r = 605.05$ g/mol): C, 41.69; H, 7.83; N, 6.94. Found: C, 41.69; H, 8.14; N, 6.73. ESI MS in MeOH (negative): m/z 353 [RuCl₃NO(L-Val)]⁻, 317 [RuCl₂NO(L-Val)-HCl]⁻, 281 [RuClNO(L-Val)-2HCl]⁻. IR, cm^{-1} : 806, 894, 1012, 1180, 1299, 1372, 1467, 1663, 1852, 2878, 2962 and 3187. UV-vis (buffer), λ_{\max} , nm (ϵ , $M^{-1}cm^{-1}$): 279 (1883), 453 (104). 1H NMR (500.32 MHz, d_6 -DMSO): δ 0.86 (d, 3H, H₆, $J = 7.9$ Hz), 0.95 (t, 12H_D, $J = 7.4$ Hz), 0.99 (d, 3H, H₅, $J = 7.9$), 1.32 (sxt, 8H_C, $J = 7.4$ Hz), 1.58 (qui, 8H_B, $J = 7.8$ Hz), 2.19 (m, 1H, H₄), 3.17 (t, 8H_A, $J = 8.2$ Hz), 3.44 (m, 1H, H₂), 4.67 (m, 1H, H₃), 6.44 (m, 1H, H_{3'}) ppm.

(Bu₄N)[RuCl₃NO(L-Ala)] (6). A mixture of Na₂[RuCl₅NO]·6H₂O (400 mg, 0.86 mmol), Bu₄NCl (450 mg, 1.62 mmol) and L-alanine (115 mg, 1.29 mmol) was refluxed in *n*-butanol (10 mL) for 1.5 h. The solvent was removed under reduced pressure and the remaining oil was dried *in vacuo*. Water (7 mL) was added. The solution was decanted into a beaker and allowed to stand at room temperature. Five days later orange crystals were filtered off and a second fraction was collected two days later. The product was washed with water/ethanol 50 : 50, diethyl ether and dried *in vacuo*. Yield: 102 mg, 21%. Anal. Calcd for C₁₉H₄₂Cl₃N₃O₃Ru ($M_r = 567.98$ g/mol): C, 40.18; H, 7.45; N, 7.40. Found: C, 40.15; H, 7.72; N, 7.05. ESI MS in MeOH (negative): m/z 324 [RuCl₃NO(L-

Ala)]⁻, 288 [RuCl₂NO(L-Ala)-HCl]⁻, 252 [RuClNO(L-Ala)-2HCl]⁻. IR, cm⁻¹: 873, 1181, 1266, 1224, 1470, 1577, 1666, 1858, 2874, 2960, 3120 and 3190. UV-vis (buffer), λ_{max}, nm (ε, M⁻¹cm⁻¹): 279 (1857), 453 (104). ¹H NMR (500.32 MHz, d₆-DMSO): δ 0.95 (t, 12H_D, J = 7.4 Hz), 1.32 (m, 12H, 8H_C, 3H₄), 1.58 (qui, 8H_B, J = 7.8 Hz), 3.17 (t, 8H_A, J = 8.2 Hz), 3.59 (qua, 1H, H₂, J = 7.3 Hz), 5.28 (m, 1H, H₃[·]) and 6.39 (m, 1H, H₃[·]) ppm.

(Bu₄N)[RuCl₃NO(L-Thr)] (7). A mixture of Na₂[RuCl₅NO]·6H₂O (400 mg, 0.86 mmol), Bu₄NCl (450 mg, 1.62 mmol) and L-threonine (154 mg, 1.29 mmol) was refluxed in *n*-butanol (10 mL) for 1.5 h. The solvent was removed under reduced pressure and the remaining oil was dried *in vacuo*. The remaining oil was dissolved in water (10 mL). The solution was decanted into a beaker and allowed to stand at room temperature. Six days later orange crystals were filtered off and a second fraction was collected three days later. The product was washed with water/ethanol 50 : 50, diethyl ether and dried *in vacuo*. Yield: 88 mg, 17%. Anal. Calcd for C₂₀H₄₄Cl₃N₃O₄Ru (M_r = 598.01 g/mol): C, 40.17; H, 7.42; N, 7.03. Found: C, 40.02; H, 7.81; N, 6.78. ESI MS in MeOH (negative): *m/z* 355 [RuCl₃NO(L-Thr)]⁻. IR, cm⁻¹: 592, 742, 890, 1066, 1173, 1257, 1372, 1459, 1642, 1849, 2875, 2966, 3233 and 3440. UV-vis (buffer), λ_{max}, nm (ε, M⁻¹cm⁻¹): 279 (1761), 453 (89). ¹H NMR (500.32 MHz, d₆-DMSO): δ 0.95 (t, 12H_D, J = 7.4 Hz), 1.17 (d, 3H; H₅, J = 6.75), 1.32 (sxt, 8H_C, J = 7.4 Hz), 1.58 (qui, 8H_B, J = 7.8 Hz), 3.17 (t, 8H_A, J = 8.2 Hz), 4.15 (m, 1H, H₄), 4.92 (m, 1H, H₃[·]), 5.16 (d, 1H, H₂, J = 5.33), 6.46 (m, 1H, H₃[·]) ppm.

(Bu₄N)[RuCl₃NO(L-Ser)] (8). A mixture of Na₂[RuCl₅NO]·6H₂O (400 mg, 0.86 mmol), Bu₄NCl (450 mg, 1.62 mmol) and L-serine (137 mg, 1.29 mmol) was refluxed in *n*-butanol (10 mL) for 1.5 h. The solvent was removed under reduced pressure and the remaining oil was dried *in vacuo*. The remaining oil was dissolved in water (10 mL). The solution was decanted into a beaker and allowed to stand at room temperature. Four days later orange crystals were filtered off. A second fraction was collected three days later. The product was washed with water/ethanol 50 : 50, diethyl ether and dried *in vacuo*. Yield: 111 mg, 22%. Anal. Calcd for C₁₉H₄₂Cl₃N₃O₄Ru (M_r = 583.98 g/mol): C, 39.08; H, 7.25; N, 7.20. Found: C, 39.30; H, 6.90; N, 6.93. ESI MS in MeOH (negative):

m/z 342 [RuCl₃NO(L-Ser)]⁻, 306 [RuCl₂NO L-Ser)-HCl]⁻, 270 [RuClNO(L-Ser)-2HCl]⁻. IR, cm⁻¹: 878, 1070, 1369, 1477, 1644, 1855, 2875, 2956 and 3448. UV-vis (buffer), λ_{max}, nm (ε, M⁻¹cm⁻¹): 279 (1721), 453 (87). ¹H NMR (500.32 MHz, d₆-DMSO): δ 0.95 (t, 12H_D, $J = 7.4$ Hz), 1.32 (sxt, 8H_C, $J = 7.4$ Hz), 1.58 (qui, 8H_B, $J = 7.8$ Hz), 3.17 (t, 8H_A $J = 8.2$ Hz), 3.59 (m, 1H, H₄'), 3.75 (m, 1H, H₄''), 4.98 (m, 1H, H₃'), 5.05 (t, 1H, H₂, $J = 5.35$ Hz), 6.45 (m, 1H, H₃'') ppm.

Physical measurements.

¹H NMR. ¹H NMR spectra were recorded on two Bruker Avance III instruments (Ultrashield Magnet) at 500.13 MHz at room temperature. DMSO-*d*₆ was used as solvent. Standard pulse programs were applied. ¹H chemical shifts were measured relatively to the solvent peaks.

ATR-IR. ATR-IR spectra were measured on a Bruker Vertex spectrometer.

Distribution coefficients. A Sanyo centrifuge was used to determine the distribution coefficient *D*. *D* values were determined by the traditional shake-flask method in *n*-octanol/buffered aqueous solution at pH 7.4 (HEPES buffer) at 298.0 ± 0.2 K as described previously.²⁰ In the case of the complexes of L-Ala (**6**) and L-Val (**5**) the *D*_{7.4} values were determined in the presence of 0.1 M KCl as well. Two parallel experiments were performed for each sample. The complexes were dissolved at 3.0·10⁻⁴ M in the *n*-octanol pre-saturated aqueous solution of the buffer (0.02 M). The aqueous solutions and *n*-octanol with 1:1 phase ratio were gently mixed with 360° vertical rotation for 3 h to avoid the emulsion formation, and the mixtures were centrifuged at 5000 rpm for 3 min by a temperature controlled centrifuge at 298 K. After separation UV spectra of the complexes in the aqueous phase were compared to those of the original aqueous solutions, and *D*_{7.4} values were calculated as the mean of [Absorbance (original solution) / Absorbance (aqueous phase after separation) – 1] obtained in the region of λ ~ (250-290 nm).

UV-vis and CD spectra. CD and UV-vis spectra under physiological conditions (0.02 M phosphate buffer, pH 7.40 with 0.1 M KCl) were recorded on a Jasco J-815 spectrometer in an optical cell of 2 cm path length in the wavelength interval from 220 to 600 nm. The analytical concentration for the CD measurement of the complexes was 50

μM in aqueous solution. Spectra were recorded in the wavelength interval from 220 to 600 nm. CD data are given as the differences in molar absorptivities between left and right circularly polarized light, based on the concentration of the ligand ($\Delta\varepsilon = \Delta A / l / c_{\text{complex}}$). The concentrations for the UV-vis measurements amounted 403 (**1**), 401 (**2**), 401 (**3**), 400 (**4**), 399 (**5**), 401 (**6**), 403 (**7**) and 401 (**8**) μM .

ESI MS. Electrospray ionization mass spectrometry (ESI MS) was carried out with a Bruker Esquire 3000 instrument; the samples were dissolved in methanol.

Electrochemistry. Cyclic voltammetry measurements were performed at room temperature using an AMEL 7050 all-in one potentiostat. The concentrations amounted 1.5-2.5 mM, the samples were dissolved in acetonitrile and NBu_4BF_4 : 0.1 to 0.2 M was added as electrolyte. Further a 3 mm GC (glassy carbon electrode) working electrode, a Pt auxiliary electrode and a SCE (saturated calomel electrode) reference electrode were used. The compartment of auxiliary electrode was separated from the study compartment. Same electrodes were used for coulometry. Ferrocene was used as an internal standard.

Structure determination. X-ray diffraction measurements were performed on a Bruker X8 APEXII CCD diffractometer. Single crystals were positioned at 40 mm from the detector and measured over 1° scan width. Exposure time and collected frames are quoted in Table 1.

Table 1. Frames collected and exposure time for **1-8**.

compound	frames	time [s]
1	1348	30
2	2183	20
3	961	10
4	1391	30
5	1100	80
6	1526	30
7	2191	30
8	2191	60

The data were processed using SAINT software.²¹ Crystal data, data collection parameters, and structure refinement details are given in Tables 2-4. The structure was solved by direct methods and refined by full-matrix least-squares techniques. Non-H atoms were refined with anisotropic displacement parameters. H atoms were inserted in calculated positions and refined with a riding model. The following computer programs and hardware were used: structure solution, *SHELXS-97* and refinement, *SHELXL-97*²²; molecular diagrams, ORTEP²³; computer, Intel CoreDuo.

Table 2. Crystal Data and Details of Data Collection for (Bu₄N)[RuCl₃NO(L)] complexes.

compound	1	2	3
empirical formula	C ₁₈ H ₃₈ Cl ₃ N ₃ O ₃ Ru	C ₂₁ H ₄₄ Cl ₃ N ₃ O ₃ Ru	C ₂₁ H ₄₄ Cl ₃ N ₃ O ₃ Ru
fw	553.96	593.01	593.01
space group	<i>Pna</i> 2 ₁	<i>P</i> 2 ₁ 2 ₁ 2 ₁	<i>P</i> 2 ₁ 2 ₁ 2 ₁
<i>a</i> , [Å]	10.1942(5)	10.2263(4)	10.1919(19)
<i>b</i> , [Å]	16.8268(9)	15.6517(6)	15.628(3)
<i>c</i> , [Å]	15.6678(8)	17.9281(7)	17.930(4)
α , [°]	90	90	90
β , [°]	90	90	90
γ , [°]	90	90	90
<i>V</i> [Å ³]	2687.6(2)	2869.55(19)	2855.9(10)
<i>Z</i>	4	4	4
λ [Å]	0.71073	0.71073	0.71073
ρ_{calcd} , [g cm ⁻³]	1.364	1.375	1.382
crystal size, [mm ³]	0.08 · 0.07 · 0.05	0.2 · 0.18 · 0.1	0.3 · 0.05 · 0.03
<i>T</i> [K]	110(2)	110(2)	120.15
μ , [mm ⁻¹]	0.90	0.85	0.85
<i>R</i> ₁ ^a	0.0362	0.0147	0.0539
<i>wR</i> ₂ ^b	0.1010	0.0418	0.1326
Flack parameter	-0.026(19)	0.015(16)	0.05(6)
GOF ^c	1.1490	1.0250	1.0100

^a $R_1 = \sum ||F_o| - |F_c|| / \sum |F_o|$. ^b $wR_2 = \{\sum [w(F_o^2 - F_c^2)^2] / \sum [w(F_o^2)^2]\}^{1/2}$. ^c $GOF = \{\sum [w(F_o^2 - F_c^2)^2] / (n - p)\}^{1/2}$, where *n* is the number of reflections and *p* is the total number of parameters refined.

Table 3. Crystal Data and Details of Data Collection for (Bu₄N)[RuCl₃NO(L)] complexes.

compound	4	5	6
empirical formula	C ₂₅ H ₄₆ N ₃ O ₄ Cl ₃ Ru	C ₂₁ H ₄₄ Cl ₃ N ₃ O ₃ Ru	C ₁₉ H ₄₂ Cl ₃ N ₃ O ₃ Ru
fw	660.08	598.01	567.98
space group	<i>P</i> 2 ₁ 2 ₁ 2 ₁	<i>P</i> 2 ₁ 2 ₁ 2 ₁	<i>P</i> 2 ₁
<i>a</i> , [Å]	9.9542(3)	8.6937(8)	15.3062(8)
<i>b</i> , [Å]	17.1180(6)	13.8069(12)	17.0885(8)
<i>c</i> , [Å]	17.8215(6)	22.7110(2)	31.3660(16)
α , [°]	90	90	90
β , [°]	90	90	91.371
γ , [°]	90	90	90
<i>V</i> [Å ³]	3036.71	2726.17 (4)	8201.7(7)
<i>Z</i>	4	4	2
λ [Å]	0.71073	0.71073	0.71073
ρ_{calcd} , [g cm ⁻³]	1.493	1.447	1.381
cryst size, [mm ³]	0.2 · 0.1 · 0.07	0.15 · 0.05 · 0.05	0.2 · 0.15 · 0.05
<i>T</i> [K]	120	100	100
μ , [mm ⁻¹]	0.814	0.89	0.889
<i>R</i> ₁ ^a	0.0337	0.0638	0.0568
<i>wR</i> ₂ ^b	0.0984	0.1646	0.1201
Flack parameter	-0.01(3)	0.00(3)	
GOF ^c	1.0375	1.1130	1.211

^a $R_1 = \Sigma ||F_o| - |F_c|| / \Sigma |F_o|$. ^b $wR_2 = \{\Sigma [w(F_o^2 - F_c^2)^2] / \Sigma [w(F_o^2)^2]\}^{1/2}$. ^c GOF = $\{\Sigma [w(F_o^2 - F_c^2)^2] / (n - p)\}^{1/2}$, where *n* is the number of reflections and *p* is the total number of parameters refined.

Table 4. Crystal Data and Details of Data Collection for (Bu₄N)[RuCl₃NO(L)] complexes.

compound	7	8
empirical formula		C ₁₉ H ₄₂ Cl ₃ N ₃ O ₄ Ru
fw	598.01	583.98
space group	<i>P</i> 2 ₁ 2 ₁ 2 ₁	<i>P</i> 1
<i>a</i> , [Å]	9.9542(3)	9.7963(4)
<i>b</i> , [Å]	17.1180(6)	10.7133(4)
<i>c</i> , [Å]	17.8215(6)	13.6446(6)
<i>α</i> , [°]	90	75.440(2)
<i>β</i> , [°]	90	85.146(2)
<i>γ</i> , [°]	90	79.953(2)
<i>V</i> [Å ³]	3036.71	1363.52(10)
<i>Z</i>	4	1
<i>λ</i> [Å]	0.71073	0.71073
<i>ρ</i> _{calcd} , [g cm ⁻³]	1.493	1.425
cryst size, [mm ³]	0.2 · 0.1 · 0.07	0.15 · 0.1 · 0.08
<i>T</i> [K]	120	100
<i>μ</i> , [mm ⁻¹]	0.814	0.896
<i>R</i> ₁ ^a	0.0337	0.0212
<i>wR</i> ₂ ^b	0.0984	0.0473
Flack parameter	-0.01(3)	-0.005(6)
GOF ^c	1.0375	1.039
$F_c^2/\Sigma[w(F_o^2)]^{1/2}$. ^c GOF = $\{\Sigma[w(F_o^2 - F_c^2)^2]/(n - p)\}^{1/2}$,		
where <i>n</i> is the number of reflections and <i>p</i> is the total number of parameters refined.		

Cell lines and culture conditions. CH1 (ovarian carcinoma, human) cells were donated by Llyod R. Kelland (CRC Center for Cancer Therapeutics, Institute of Cancer Research, Sutton, U.K.). SW480 (colon adenocarcinoma, human) cells and A549 (non-small cell lung cancer) were kindly provided by Brigitte Marian (Institute of Cancer Research, Department of Medicine I, Medical University of Vienna, Austria). Cells were grown without antibiotics in 75 cm² culture flasks (Iwakai/Asahi Techoglass) and adherent monolayer cultures in Minimal Essential Medium (MEM) supplemented with 10% heat inactivated fetal bovine serum, 1 mM sodium pyruvate and 2 mM L-glutamine

(all purchased from Sigma Aldrich). Cultures were maintained at 37 °C in a humidified atmosphere containing 5% CO₂ and 95% air.

Cytotoxicity in cancer cell lines. Colorimetric MTT assays (MTT = 3-(4,5-dimethyl-2-thiazolyl)-2,5-diphenyl-2H-tetrazolium bromide, purchased from Sigma Aldrich) were performed in the cell lines mentioned above to evaluate cytotoxicity. Cells were harvested from culture flasks by trypsinization and seeded in 100 µL aliquots in MEM supplemented with the chemicals mentioned above and 1% non-essential amino acids (all purchased from Sigma Aldrich) into 96-well microculture plates. (Iwaki/Asahi Technoglass). The following cell densities were chosen to ensure exponential growth of untreated controls through the experiment: 1.5·10³ (CH1), 2.5·10³ (SW480), 4.0·10³ (A549) viable cells per well. Cells were allowed to settle and resume exponential growth for 24 h, followed by the addition of dilutions of the test compounds in aliquots of 100 µL/well in the same medium. The cells were exposed continuously for 96 h, then the medium was replaced by 100 µL/well RPMI medium supplemented with 10% heat inactivated fetal bovine serum and 4 mM L-glutamine plus 20 µL/well solution of MTT in phosphate-buffered saline (5 mg/mL) (all purchased from Sigma Aldrich). It was incubated for 4 h and medium/MMT mixtures were removed. The formazan product formed by the viable cells was dissolved in DMSO (150 µL/well). Optical densities at 550 nm were measured with a microplate reader (Tecan Spectra Classic), using a reference wavelength of 690 nm to correct for unspecific absorption. The quantity of viable cells was expressed as percentage of untreated controls, and 50% inhibitory concentrations (IC₅₀) were calculated from concentration-effect curves by interpolation. Evaluation is based on at least three independent experiments, each comprising three replicates per concentration level.

Results and Discussion

Synthesis and characterization of (Bu₄N)[RuCl₃NO(L)] complexes.

Na₂[RuCl₅NO]·H₂O was prepared by a reaction of RuCl₃·H₂O with NO released from NaNO₂ in 40% yield.¹⁸ In the second step Na₂[RuCl₅NO]·H₂O was refluxed with 1.5 equiv Bu₄NCl and 1.1 equivalent of the amino acid in *n*-butanol. After 30 min, the color

changed from violet to red-brown. The reaction time was varied from 1 to 12 h, but no differences were observed. In the case of glycine (**1**) and L-tyrosine (**4**) the product was crystallized directly from the mother liquor. For the other complexes the *n*-butanol was evaporated and the residue was dissolved in water, a concentration of 100 mM turned out to be appropriate. Crystallization worked best in 50 mL Erlenmeyer flasks and took four days on average at room temperature. The positive ESI mass spectra of all complexes showed only presence of two peaks at *m/z* 242 and 518 associated to $[\text{Bu}_4\text{N}]^+$ and $[\text{Bu}_4\text{N} + \text{Bu}_4\text{NCl}]^+$. In the negative ion mode the peaks with the highest intensity could be attributed to the complex anions $[\text{RuCl}_3\text{NO}(\text{L})]^-$, peaks with moderate intensities assigned to $[\text{RuCl}_2\text{NO}(\text{L})\text{-HCl}]^-$ and $[\text{RuClNO}(\text{L})\text{-2HCl}]^-$ usually also were found. All complexes are soluble in DMSO. The stability in DMSO over 24 h was proved by ^1H NMR spectroscopy. ATR-IR spectra of all complexes were recorded and the nearly linear binding of a NO^0 or NO^+ moiety could be confirmed by an intense characteristic band between 1837 for the glycine complex (**1**) and 1852 cm^{-1} for the L-tyrosine complex (**4**) cm^{-1} . The NO band of the educt $\text{Na}_2[\text{RuCl}_5\text{NO}]$ was found at 1902 cm^{-1} .

Crystal structures. The crystal structures of the complex anions with aliphatic amino acids, (**1**, **5** and **6**) are displayed in Figure 14. Figure 15 displays the proline complexes **2** and **3**. The complex anion of **4** is shown in Figure 16. The crystal structure of the complex **8** with L-serine is displayed in Figure 17.

As can be seen the carboxyl group is always found in *trans* position to the NO. As expected from the IR spectra the NO is bound to ruthenium via the nitrogen. The Ru-NO entity is almost linear and the Ru-NO bond length is about 1.71 \AA . The chlorido ligands are bound meridionally other and have with about 2.37 \AA a typical bond length. The Ru-O bond length is about 2.0 \AA . Selected bond lengths are given in Table 5. The bond angles Ru-N2-O3, N2-Ru-O1 and N2-Ru-Cl1 are listed in Table 6. There are no large geometrical parameters variation among the complexes. The five-membered rings (Ru-N1-C1-C2-O1) are almost planar, the torsion angles Ru-N1-C1-C2 are quoted in Table 7.

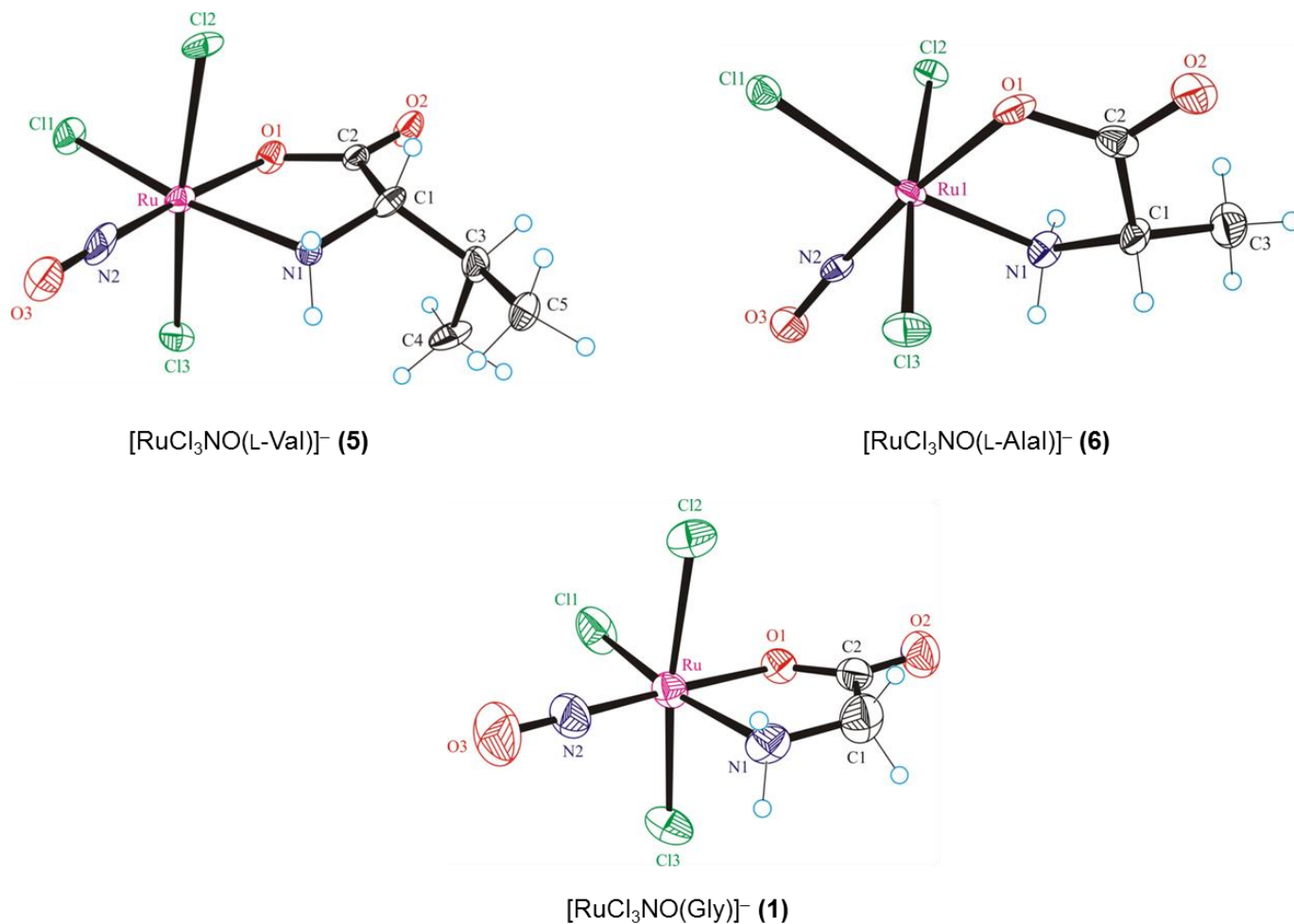


Figure 14. Crystal structures of the complex anions containing aliphatic AA.

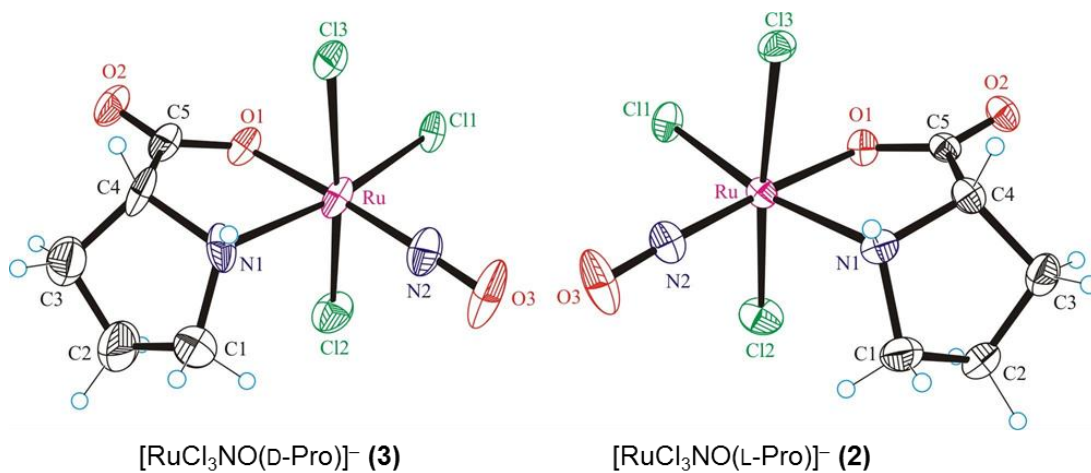


Figure 15. Crystal structures of D-Pro (3) and L-Pro (2) complexes.

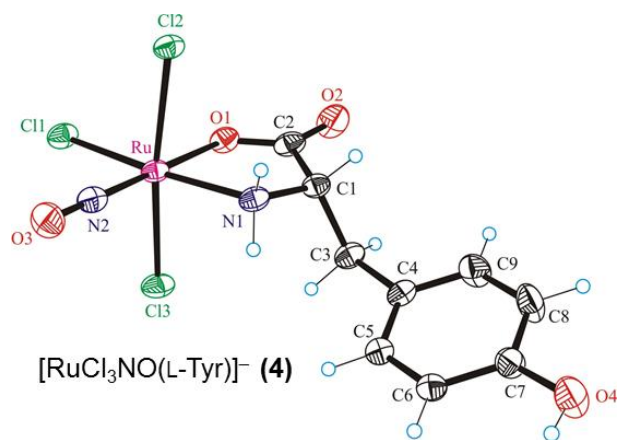


Figure 16. Crystal structures of L-Tyr (**4**) complexes.

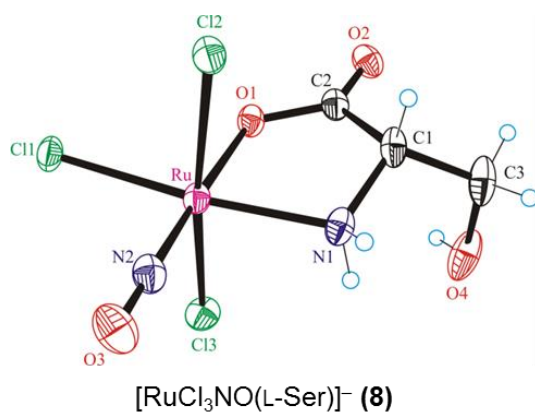


Figure 17. Structures of the complex anion of **8**.

Table 5. Selected bond lengths (Å) for the complexes 1–8.

bond	1	2	3	4	5	6	7	8
Ru-N2	2.061(6)	2.072(15)	2.132(6)	2.081(2)	2.103(9)	2.081(10)	2.088(3)	2.0688(15)
Ru-N1	1.705(7)	1.726(6)	1.726(6)	1.731(2)	1.727(10)	1.727(14)	1.730(3)	1.7267(16)
Ru-O1	2.004(5)	1.9982(11)	1.988(4)	2.0174(9)	1.996(7)	1.975(7)	2.011(3)	2.0074(13)
Ru-Cl1	2.379(18)	2.3756(4)	2.383(18)	2.376(2)	2.363(3)	2.371(3)	2.3761(9)	2.3697(4)
N2-O3	1.145(10)	1.147(2)	1.141(7)	1.138(3)	1.151(11)	1.1351(14)	1.144(4)	1.149 (2)

Table 6. Selected bond angles (°) for the complexes 1–8.

angel (°)	1	2	3	4	5	6	7	8
Ru-N2-O3	180.01(11)	176.52(16)	176.40(6)	179.10(3)	177.83(8)	178.21(4)	174.10(3)	178.47(15)
N2-Ru-O1	176.75(3)	177.09(7)	177.43(3)	177.28(11)	174.12(4)	176.01(4)	173.45(13)	176.68(16)
N2-Ru-Cl1	93.92(1)	93.27(4)	93.02(7)	93.30(8)	93.23(4)	92.22(4)	95.69(11)	93.38(5)

Table 7. Selected torsion angles (Ru-N1-C1-C2) (°) for the complexes 1–8.

torsion angle (°)	1	2	3	4	5	6	7	8
Ru-N1-C2-C1	6.9(8)	15.4(2)	15.0(7)	-171.4 (2)	7.0(1)	0(1)	-152.3(3)	-29.2(2)

Lipophilicity. The complexes were found to be moderately water soluble and stable in solution within the time frame of the measurements even without the presence of chloride ions as illustrated in Figure 18. It is noteworthy that hydrolysis of the complexes is negligible during 24 h in the presence of 0.1 M chloride ion.

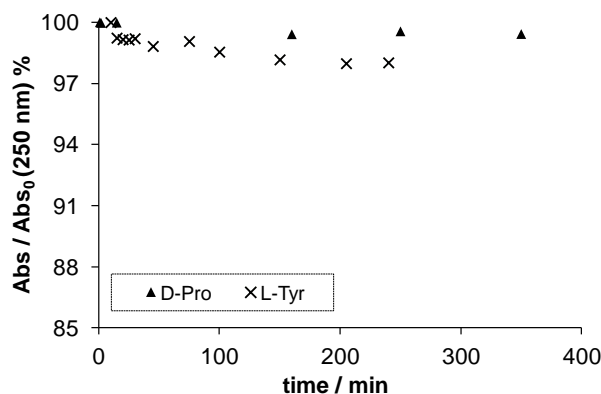


Figure 18. Time dependence of absorbance values of $(\text{Bu}_4\text{N})[\text{RuCl}_3\text{NO}(\text{L})]$ complexes, where $\text{L} = \text{L-Pro}$, D-Pro and L-Tyr recorded at 250 nm at pH 7.40 [$c_{\text{complex}} = 2.5 \times 10^{-4} \text{ M}$; 0.02 M HEPES; $T = 298.0 \text{ K}$].

The $\log D_{7.4}$ values of the complexes were determined at pH 7.40 by analysis of the UV spectra of the aqueous phases before and after separation (Fig. 19, Table 8). Results revealed the fairly hydrophilic character of all the complexes studied. The $\log D_{7.4}$ values show the following order: Gly (**1**) < L-Ser (**8**), L-Thr (**7**), L-Ala (**6**), < D/L-Pro (**3/2**), < L-Tyr (**4**), L-Val (**5**) corresponding well to the expectations based on the hydrophilicity of the side chains of the coordinated amino acids. On the other hand the presence of chloride ion does not alter significantly the lipophilicity of the complexes (Table 8).

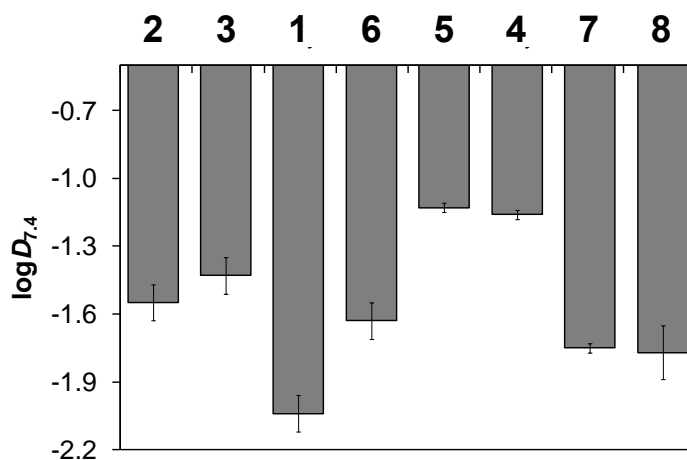


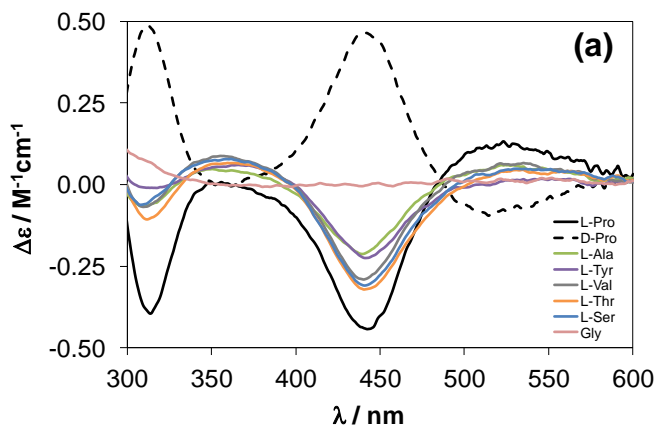
Figure 19. $\log D_{7.4}$ values of the various $(\text{Bu}_4\text{N})[\text{RuCl}_3\text{NO}(\text{L})]$ complexes [0.02 M HEPES; $T = 298.0 \text{ K}$].

Table 8. $\log D_{7,4}$ values of the various $(\text{Bu}_4\text{N})[\text{RuCl}_3\text{NO}(\text{L})]$ complexes [0.02 M HEPES; $T = 298.0$ K].

L:	$\log D_{7,4}$	$\log D_{7,4}^{[a]}$
L-Pro	-1.55 ± 0.08	
D-Pro	-1.43 ± 0.08	
Gly	-2.04 ± 0.08	
L-Ala	-1.63 ± 0.08	-1.47 ± 0.11
L-Val	-1.13 ± 0.02	-1.31 ± 0.07
L-Tyr	-1.16 ± 0.02	
L-Thr	-1.75 ± 0.02	
L-Ser	-1.77 ± 0.12	

[a] in the presence 0.1 M KCl

UV-vis and CD spectra. The complexes possess fairly similar UV-vis spectra with a well-defined λ_{max} at 452 nm (Fig. 20). CD spectra of the complexes of the L-amino acids show similarities as well, namely negative peaks with λ_{max} at ~ 440 and 313 nm, while the complex of D-Pro shows positive peaks at the same wavelength values.



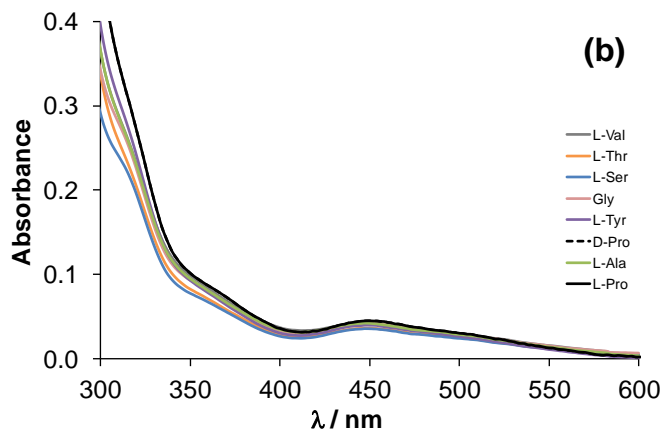


Figure 20. CD (a) and UV-vis (b) spectra of the studied $(\text{Bu}_4\text{N})[\text{RuCl}_3\text{NO}(\text{L})]$ complexes at pH 7.40 [$C_{\text{complex}} = 5.0 \times 10^{-5}$ M; 0.02 M phosphate buffer; 0.1 M KCl; $T = 298$ K].

Electrochemistry. For a series of compounds (**2**, **3**, **5**, **7**, **8**), the same electrochemical behavior was observed as shown in Figure 21-23 with a high-potential oxidation peak, divided into two waves or not, (with a $n_{\text{ox,app}}$ generally equal to 3) and a small and large reduction wave. The general pattern of reduction peaks seems to be dependent on the state of the electrode area. For the complex with L-Val (**5**), the separation of the oxidation waves is more obvious and two oxidation waves around 1.9 V/SCE and 2.3 V/SCE can be observed. Table 9 summarizes the peak potential values at 100 mV/s.

These results show that the oxidation of the ruthenium complexes involves the oxidation of the coordinated amino-acid. The high value of the electron apparent number determined by coulometry and by comparison of the peak intensity of ferrocene provides further evidence for a complex process ($n_{\text{app}} = 3$ generally).

In contrast, the monoelectronic reduction can be ascribed to the irreversible reduction of the metal center leading to a change in the complex (conformation, breaking bond ...).

Table 9: Peak potential [V] in the same conditions ($\text{CH}_3\text{CN}/(n\text{Bu}_4)\text{BF}_4$ 0.1 M): ^a determined in the experiment with several cycles of potential; ^b in comparison with the ferrocene these values are close. ^c no clear oxidation wave was observed.

compound	Oxidation peaks	Reduction peaks ^a
2	1.63 ^b	-0.79
3	1.68 ^b	-0.82
4	^c	-2.25
5	1.8 ^{sh} 1,90 2.28	-1.31
6	^c	-0.79
7	1.8 ^{sh} 1.91	-0.83
8	1.8 ^{sh} 1.87	-0.80

Sh = shoulder

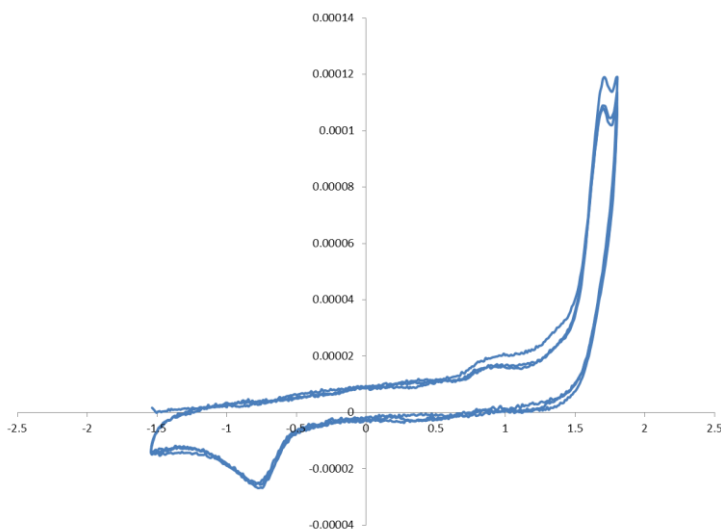


Figure 21: Cyclic voltammograms with several cycles of potential of **3** at 100 mV/s in acetonitrile on GC electrode.

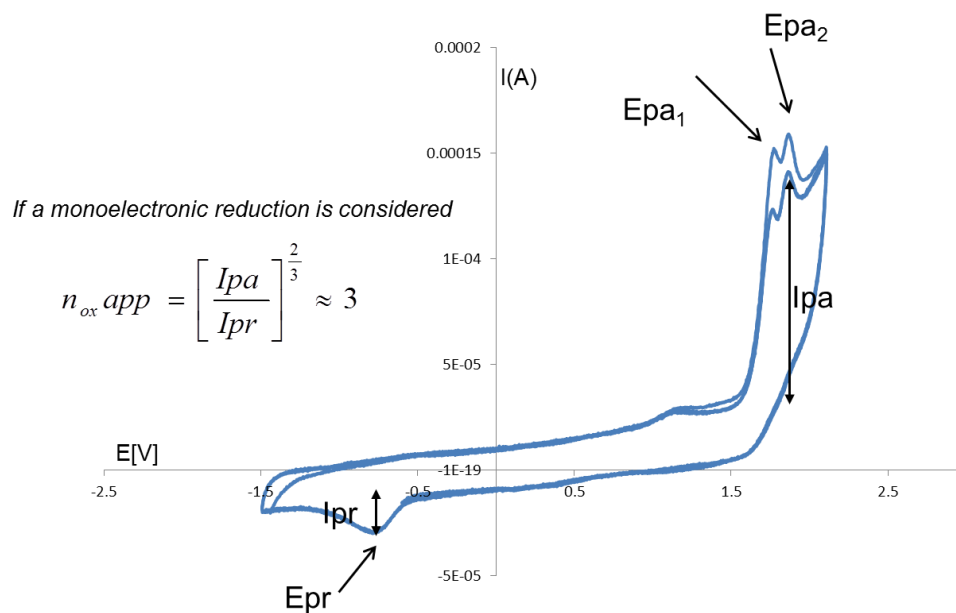


Figure 22: Cyclic voltammograms with several cycles of potential for **8** at 100 mV/s in acetonitrile on GC electrode.

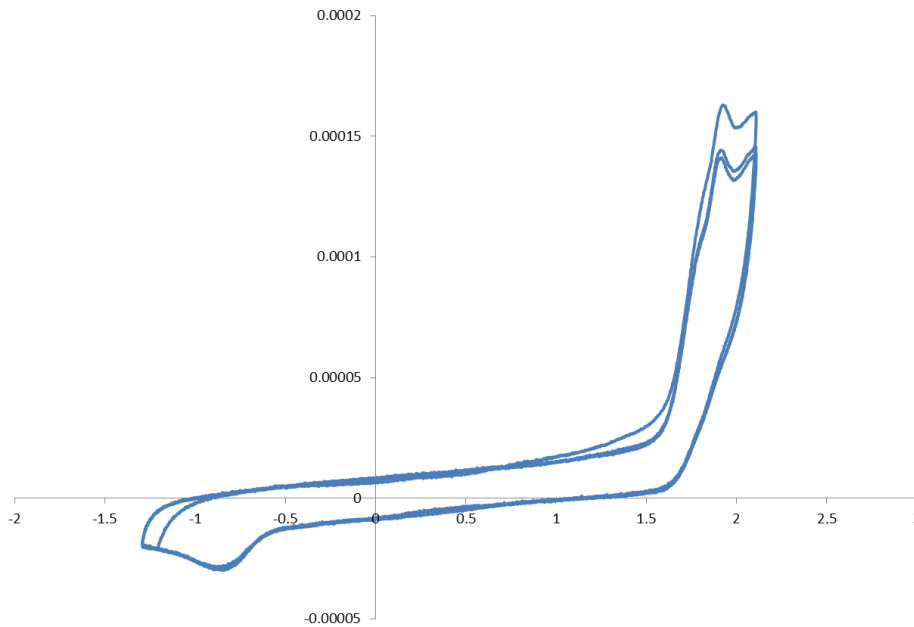


Figure 23 Cyclic voltammograms with several cycles of potential for **7** at 100 mV/s in acetonitrile on GC electrode.

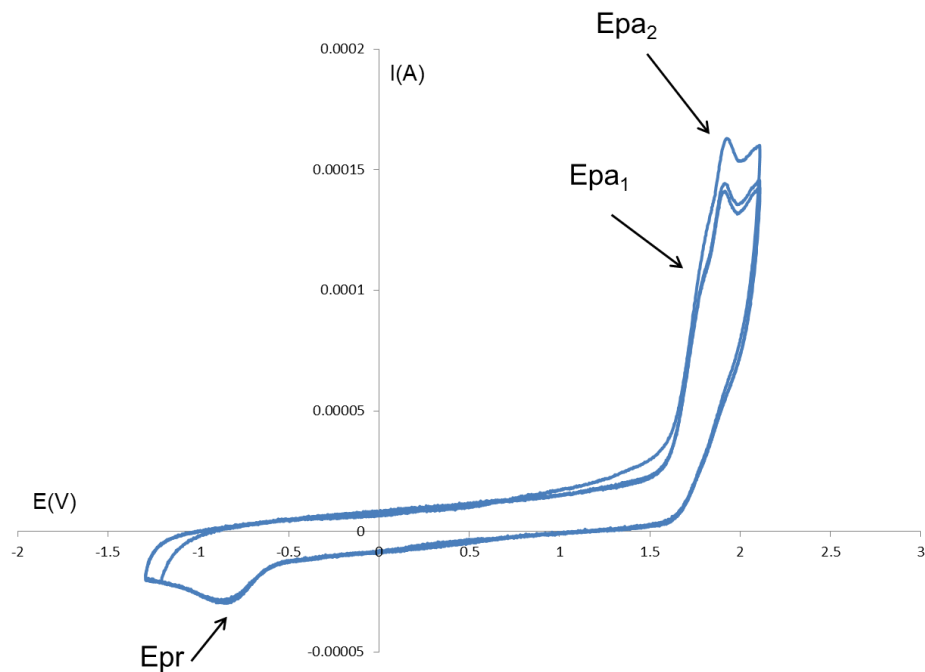


Figure 21: Cyclic voltammograms with several cycles of potential for **5** at 100 mV/s in acetonitrile on GC electrode.

Cytotoxicity in cancer cell lines. Cytotoxicity of all compounds (**1-8**) was assessed by means of a colorimetric micro culture (MTT) assay in three human cancer cell lines, namely A549 (non-small cell lung carcinoma), CH1 (ovarian cancer) and SW480 (colon adenocarcinoma). The cell line A549 is least sensitive. This cell line is known to be little chemosensitive in general. CH1 is most sensitive to the compounds and in general the most chemosensitive among these three. For CH1 the IC₅₀ is 3.6 times higher for the glycinato complex (**1**), which is the most hydrophilic compound, than for the valinato complex (**5**), which is the most hydrophobic compound. Moreover the L and the D prolinato complexes (**2,3**) showed different antiproliferative activity. The IC₅₀ values for compound **3** are 2.9 times lower in A549, 1.6 times in CH1 and 2.7 times in SW480 cells.

Tab.10. Cytotoxicity of the compounds **1-8** in three human cancer cell lines.

IC50 values ± SD			
	A549	CH1	SW480
5	>320	26.9 ± 3.4	53.2 ± 2.3
7	>320	23.1 ± 2.0	71.3 ± 15.3
6	>320	12.2 ± 2.2	46.5 ± 2.8
8	>320	12.8 ± 1.9	62.9 ± 10.2
3	108.3 ± 5.1	12.7 ± 1.0	20.0 ± 3.2
1	195.8 ± 26.7	7.5 ± 1.2	39.2 ± 3.4
4	>320	16.8 ± 2.7	38.2 ± 11.8
2	>320	20.1 ± 2.8	53.7 ± 9.8

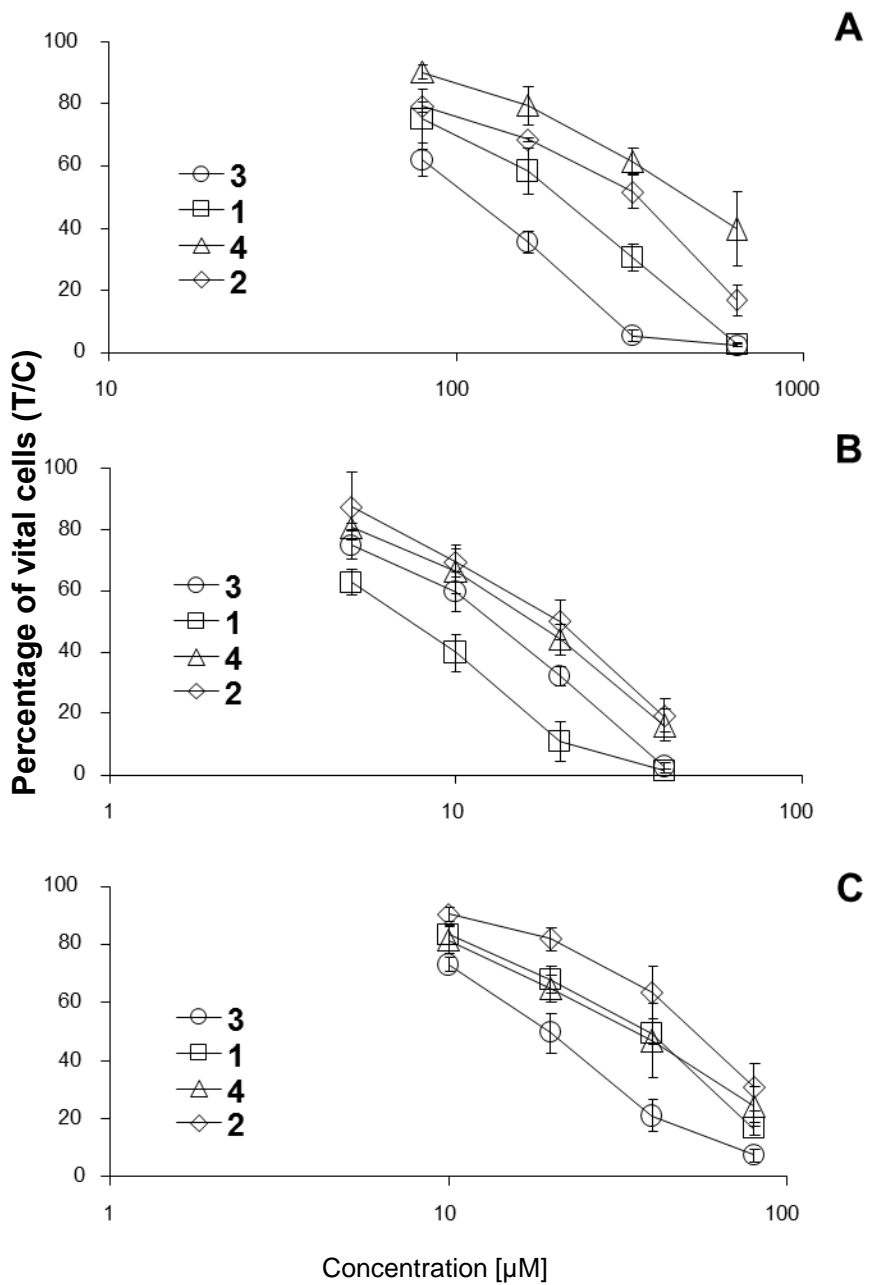


Figure 24. Concentration–effect curves of ruthenium-based complexes (**3**, **1**, **4** and **2**) in A549 (A), CH1 (B) and SW480 (C) cells, based on means \pm standard deviations of at least three independent experiments each.

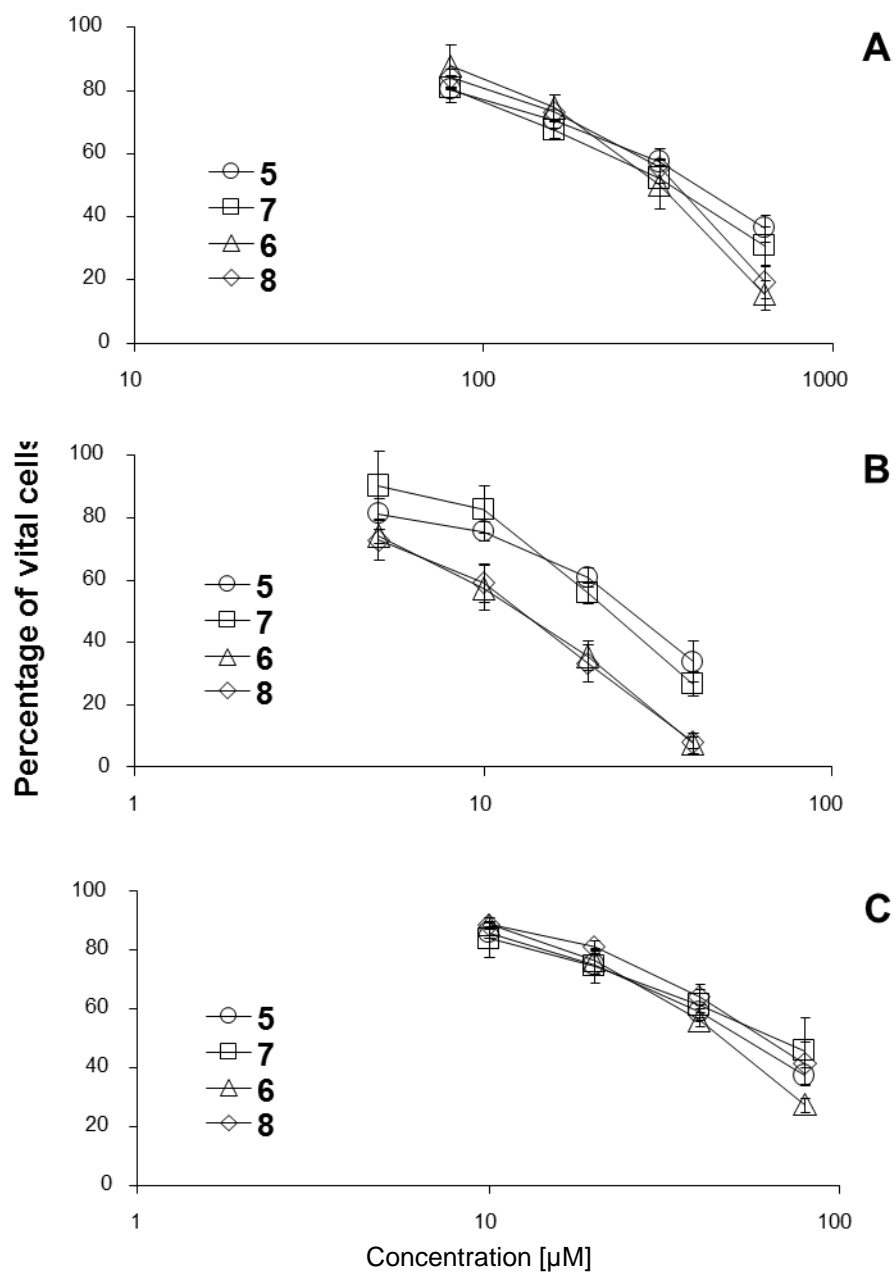


Figure 25. Concentration–effect curves of ruthenium-based complexes (**5**, **7**, **6** and **8**) in A549 (A), CH1 (B) and SW480 (C) cells, based on means \pm standard deviations of at least three independent experiments each.

2.2 Investigation of the Interaction between HSA and $[MCl_4NO(Hind)]^-$ Complexes

The interaction of Human Serum Albumin (HSA) (Fig. 27) with potential anticancer active compounds of the formula $((H_2Ind)/Na)[cis/trans-MCl_4NO(Hind)]$ (Fig. 26) was investigated and conditional stability constants ($\log K'$) were determined.

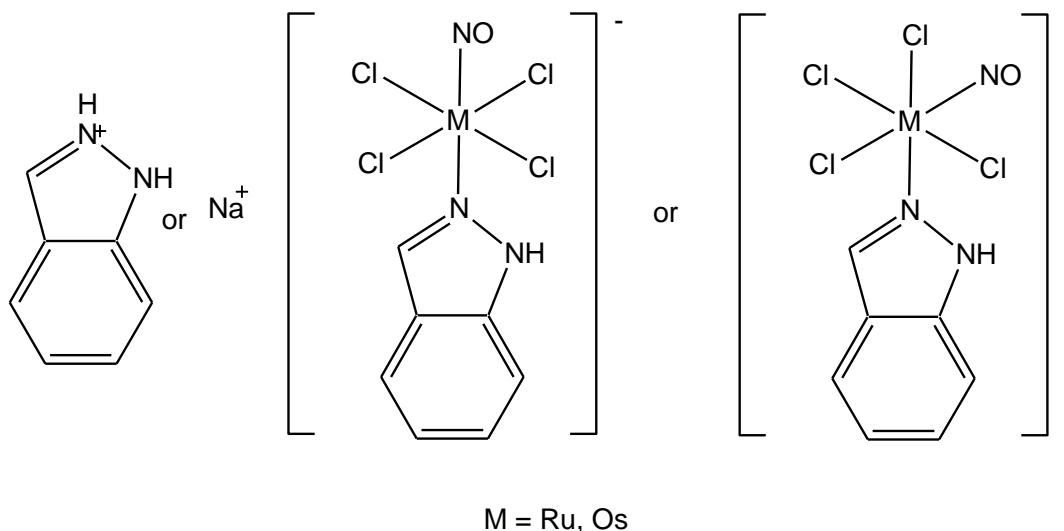


Figure 26. Compounds for which the interaction with HSA was tested.

Hydrolysis stability in 20 mM phosphate buffer (pH 7.40) containing 150 mM NaCl + 1% DMSO buffer was confirmed by several UV-vis measurements over 24 h. Then ultrafiltration measurements were performed and the remaining concentration of free complex was determined by UV-vis. In this manner it was established if the complexes bind to HSA and how many complexes HSA can bind, but these experiments did not provide any information about the binding site. The binding to site I in subdomain IIA was investigated by Warfarin displacement. Warfarin selectively binds to site I and fluoresces only if it is bound. On the same principle the binding to site II in subdomain IIA was explored by Dansyl glycine (DG) displacement. Warfarin and DG are established side markers for HSA. Furthermore Trp-214 quenching on site I was studied and the binding to SH-34 (IA) was explored by 4,4'-dithiodipyridine (DTDP) method. Interaction of the free SH-group at Cys-34 with DTDP generates a 2-TP colored product ($\lambda_{max} = 340 \text{ nm}$). If the complex (the NO-ligand) interacts with the SH-group of HSA then

the later added DTDP can interact just with the remainder SH-groups. A negative saturation curve is expected at increasing amount of complex to HSA.

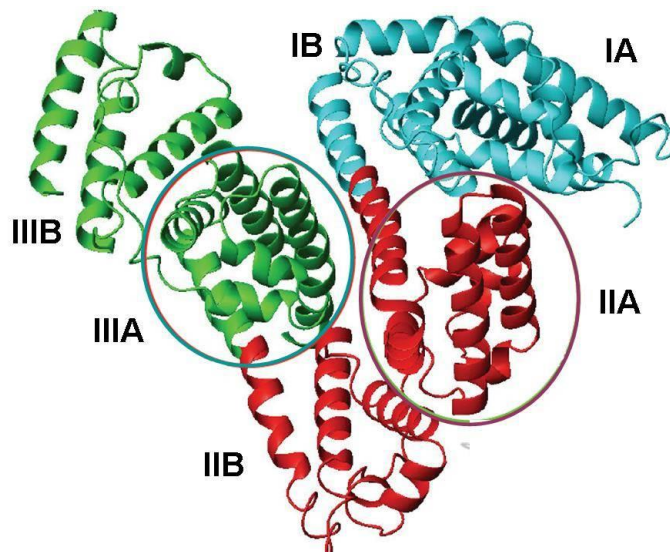


Figure 27. HSA with labeled subdomains.

Materials and methods

Chemicals. The ruthenium compounds were synthesized at the Institute of Inorganic Chemistry of the University of Vienna. The osmium compounds were synthesized at the Department of Chemistry and Biochemistry of the University of Lyon.²⁴ Racemic WF, DG, DTDP and HSA (as lyophilized powder with fatty acids, A1653), NaH_2PO_4 , Na_2HPO_4 , and NaCl were purchased from Sigma-Aldrich in puriss quality. Doubly distilled Milli-Q water was used for preparation of samples. HSA solutions were freshly prepared before the experiments and their concentrations were estimated from its UV absorption: $\epsilon_{280 \text{ nm}}(\text{HSA}) = 36,850 \text{ M}^{-1} \text{ cm}^{-1}$.²⁵ Solutions of WF and DG were prepared prior to the analyses with 1 equiv of NaOH and their concentrations were calculated on the basis of their UV-vis spectra: $\epsilon(308 \text{ nm}) \text{ WF} = 14,475 \text{ M}^{-1} \text{ cm}^{-1}$, $\epsilon(327 \text{ nm}) \text{ DG} = 5,068 \text{ M}^{-1} \text{ cm}^{-1}$.

Spectrofluorimetric measurements. Fluorescence spectra were recorded with a Hitachi-F4500 fluorimeter using a 5 nm/5 nm slit width in a 1 cm quartz cell at 25.0 ± 0.1 °C. All solutions were prepared in 20 mM phosphate buffer (pH 7.40) containing 150

mM NaCl + 1% DMSO. Samples usually contained 1 μ M HSA and various HSA-to-ligand ratios (from 1:0 to 1:20) were used. In the site marker displacement experiments, the HSA to site marker (WF or DG) ratio was 1 : 1 and the concentration of the complexes was varied. Spectra were recorded after 2 h incubation. The excitation wavelengths were 295 (Try-214), 310 (WF) or 335 (DG) nm depending on the type of experiment, and the emission was read in the range 310–650 nm. The conditional binding constants were calculated with the computer program PSEQUAD.²⁶ Three-dimensional spectra were recorded for 210–350-nm excitation and 230–450-nm emission wavelengths. A correction for self-absorbance was necessary in the quenching experiments because fluorescence is significantly absorbed by the complexes. The correction was done according to the equation, where $F_{corrected}$ and $F_{measured}$ are the corrected and measured fluorescence intensities, and $A(EX)$ and $A(EM)$ are the absorptivities at the excitation and emission wavelengths in the samples, respectively.²⁷

$$F_{corrected} = F_{measured} \times 10^{\left(\frac{A(EX)+A(EM)}{2}\right)}$$

Membrane ultrafiltration-UV-vis measurements. Samples were separated by ultrafiltration through 10 kDa membrane filters (Microcon YM-10 centrifugal filter unit, Millipore) in LMM (low molecular mass) and HMM (high molecular mass) fractions with the help of a temperature-controlled centrifuge (Sanyo, 10,000 s^{-1} , 10 min). The samples (0.50 mL) contained 60 μ M HSA and the metal complexes (from 10 to 150 μ M) in 20 mM phosphate buffer (150 mM NaCl; pH 7.40 at 25.0 \pm 0.1 $^{\circ}$ C) and were incubated for 15 min. In the site marker displacement experiments, the HSA to site marker ratio was 1 : 1 and the concentration of the complexes was varied from 10 to 180 μ M. The LMM fraction containing the nonbound metal complex was separated from HSA and HSA–complex adducts in the HMM fraction. The LMM fractions were diluted to 1.00 mL, and the concentration of the nonbound complex was determined by UV-vis spectrophotometry. The UV-vis spectra of the LMM fractions were compared with the reference spectra of the samples containing free complex without the protein at a

concentration equal to that in the ultrafiltered samples. A Hewlett-Packard 8452A spectrophotometer was used to record the spectra in the region from 200 to 700 nm at 25 °C and with a path length of 1 cm.

Results and discussion

Numbering of the compounds

1: Na[*cis*-OsCl₄NO(Hind)]

2: Na[*trans*-OsCl₄NO(Hind)]

3: Na[*trans*-RuCl₄NO(Hind)]

4: (H₂Ind)[*trans*-OsCl₄NO(Hind)]

5: (H₂Ind)[*trans*-RuCl₄NO(Hind)]

Membrane ultrafiltration-UV-vis measurements.

Table 11 displays the percentage of free complex passing through the filter. In the case of **1** only 50% passed through the filter and, therefore, this complex could not be studied further by UF experiments.

Tab. 11. Percent of free complex going through the filter.

	1	2	3	4	5
% going through the filter	50	100	94	100	100

The results of the ultrafiltration experiments under physiological conditions (150 mM NaCl; pH 7.40 at 25.0 ± 0.1 °C) are displayed in Table 12. It is obvious that more than 1 complex molecule can bind to a single HSA. In the last experiment 4 times diluted human blood serum was used. The HSA concentration in blood serum is about 650 µM, which means that the HSA concentration in the tested sample was about 160 µM.

Tab. 12. Percent of bound complex under physiological conditions.

c(HSA), c(complex), [μ M]	% bound 2	% bound 4	% bound 5	% bound 3
630 + 320 _1	92	94	92	92
630 + 320 _2	93	93	92	92
				92
630 + 270	88	-	-	
160 + 80	88	83	81	75
				82
630 + 270	88	-	-	
50 + 50	70	77	64	
Serum/4 + 80	-	-	~ 79	85
			~ 83	86

Quenching experiments

Side 1: quenching of Trp-214. The conditional stability constants for site 1 binding calculated based on Trp-214 quenching were very similar for all tested compounds (Tab.13).

Tab. 13. LogK' constants for binding side 1, calculated from Trp-214 quenching.

PSEQUAD	1	2	4	5
logK' (site I)	5.06	5.10	4.95	4.92
SD	0.01	0.01	0.03	0.03

Side 1: displacement of Warfarin. Table 14 shows the $\log K'$ constants for the compounds **1**, **2**, **4**, and **5**. They are very similar to each other and fit well to the constants obtained with Trp-214 quenching.

Tab. 14. . $\log K'$ constants for binding side 1, calculated from warfarin displacement.

PSEQUAD	1	2	4	5
$\log K'$ (site I)	4.98	5.00	5.00	4.90
SD	0.01	0.01	0.01	0.01

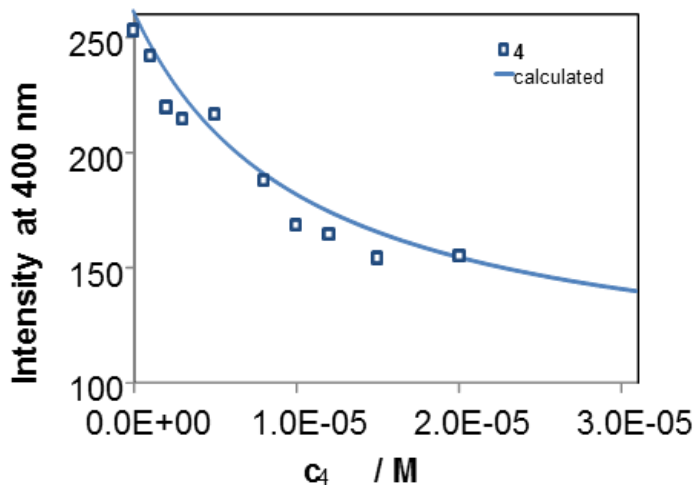


Figure 28. Intensities of warfarin fluorescence at 400 nm.

The intensities of Warfarin emission at 400 nm with increasing concentration of **4** are displayed in Figure 28. Figure 29 shows the decreasing intensity of Warfarin fluorescence, if **4** is added, at about 400 nm. At the same time it can be seen that the emission of H_2Ind^+ at 325 nm increases. Due to the strong emission of H_2Ind^+ from 305 to 355 nm this area was chosen. Unbound Warfarin does not emit.

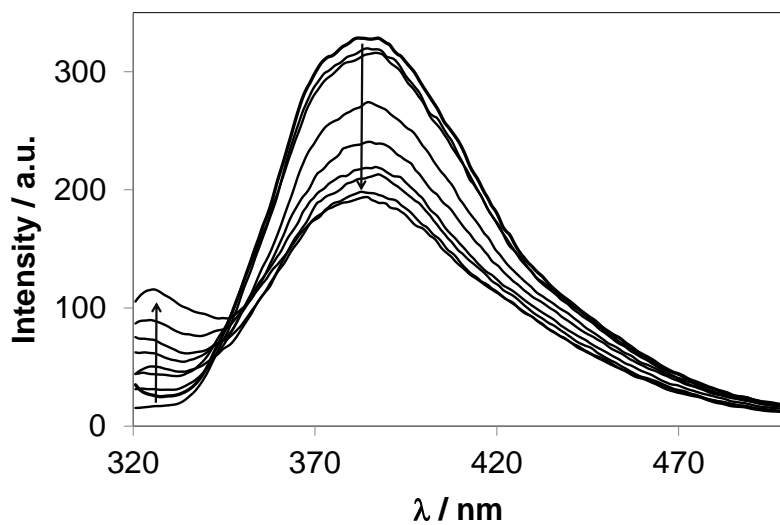


Figure 29. Warfarin quenching for 4 .

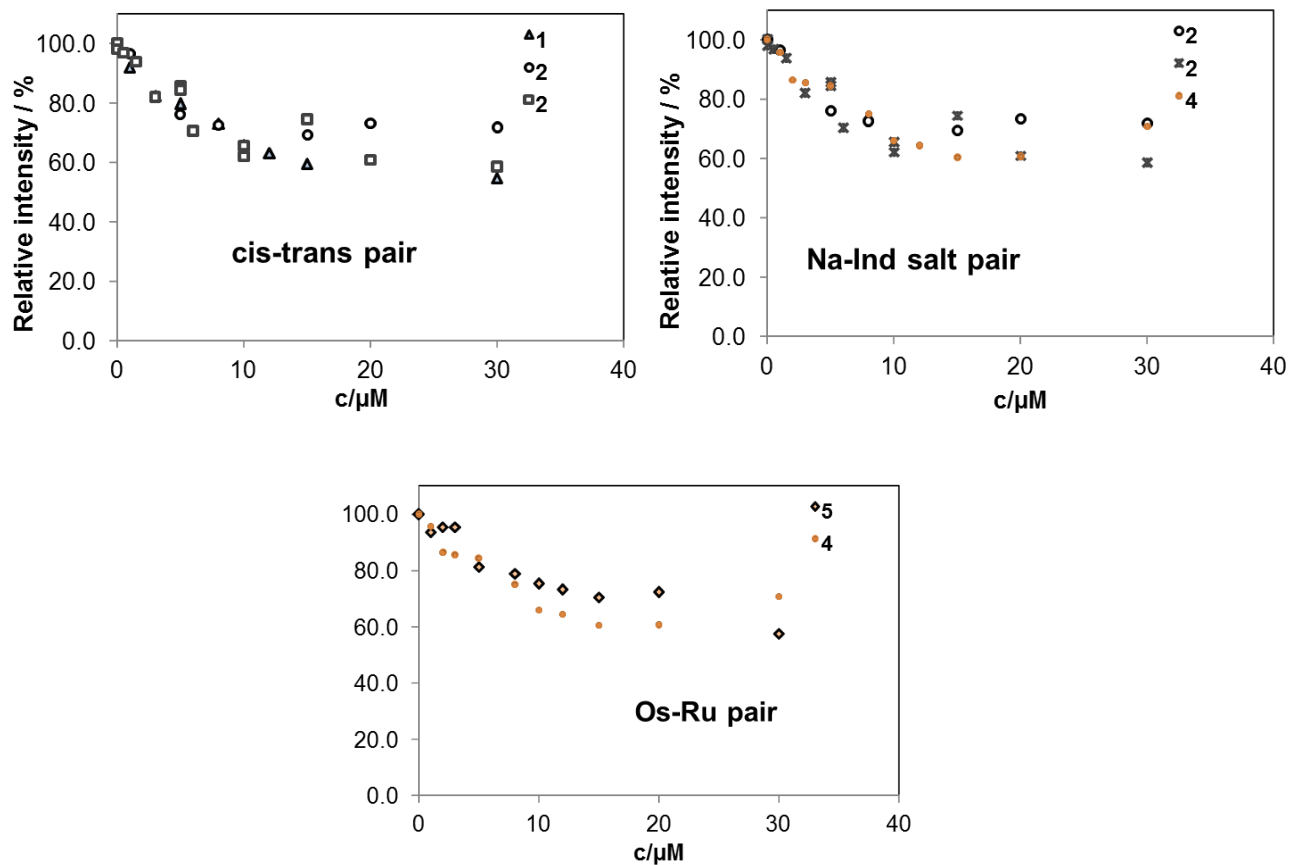


Figure 30. Intensities of warfarin emissions at 380 nm for various pairs of complexes.

The warfarin emission at 380 nm with increasing complex concentration was compared for the compounds Na[*cis*-OsCl₄NO(Hind)] (**1**), Na[*trans*-OsCl₄NO(Hind)] (**2**), the sodium (**2**) and the indazolium (**4**) salt of [*trans*-OsCl₄NO(Hind)] and for the Ru(**5**)/Os(**4**) pair of (Hind)[*trans*-OsCl₄NO(Hind)]. As expected from the logK' constants all compounds showed a very similar behavior (Fig. 30).

Side II: displacement of Dansyl glycine (DG). The logK' constants for the interaction with site II were calculated from DG displacement. The results are displayed in Table 15. The constants for 1, 2 and 5 are about 0.3 lower than the constants for site I, the constant for 4 is about 0.6 lower. All constants are in a similar range.

Tab.15. LogK' constants for binding site 1, calculated from warfarin displacement.

PSEQUAD	1	2	3	4	5
logK' (site I)	4.69	4.61	4.58	4.37	4.65
SD	0.01	0.003	0.004	0.004	0.004

Figure 31 and 32 show the decreasing DG fluorescence with increasing complex concentrations. For the graph plotted in Figure 31 the maxima of the emissions at various complex concentrations were considered.

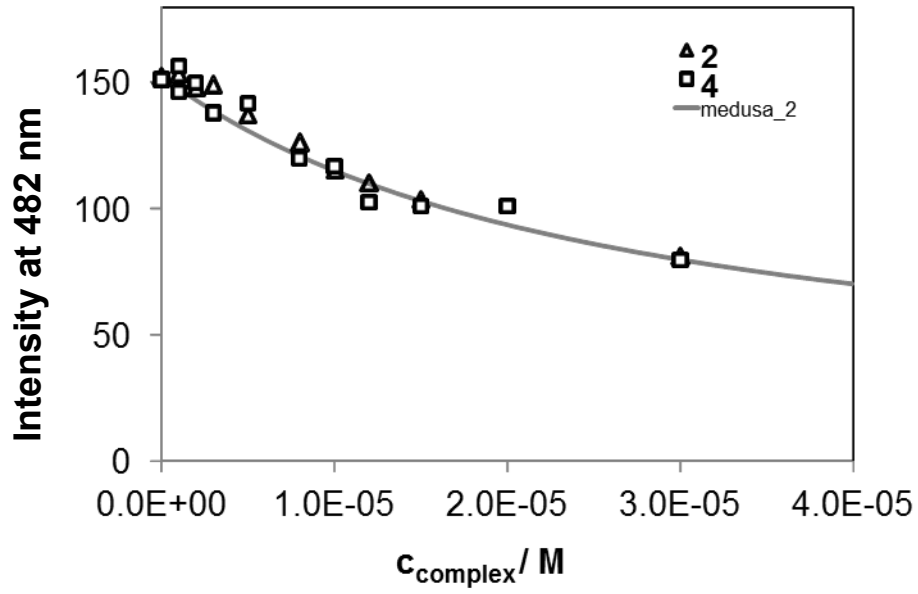


Figure 31. Intensities of DG fluorescence at 482 nm.

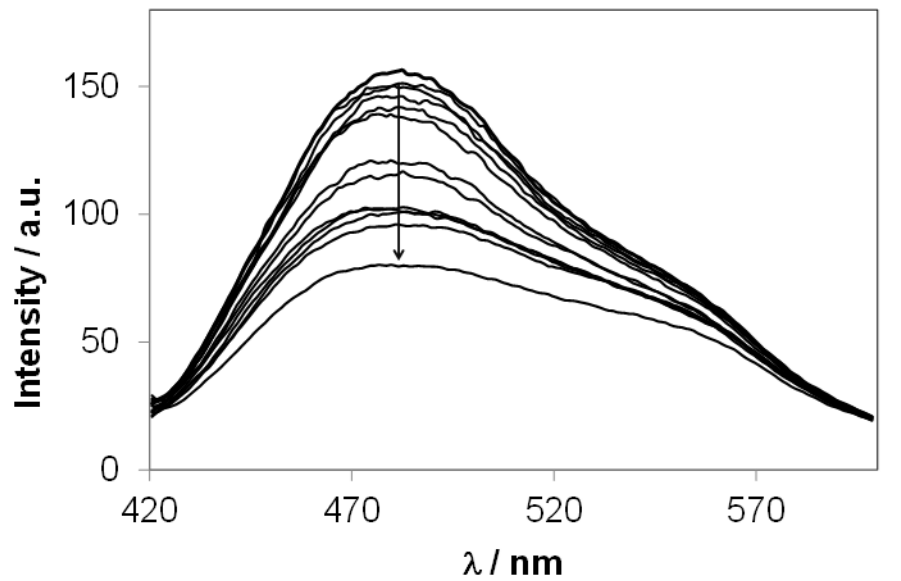


Figure 32. DG displacement 482 nm.

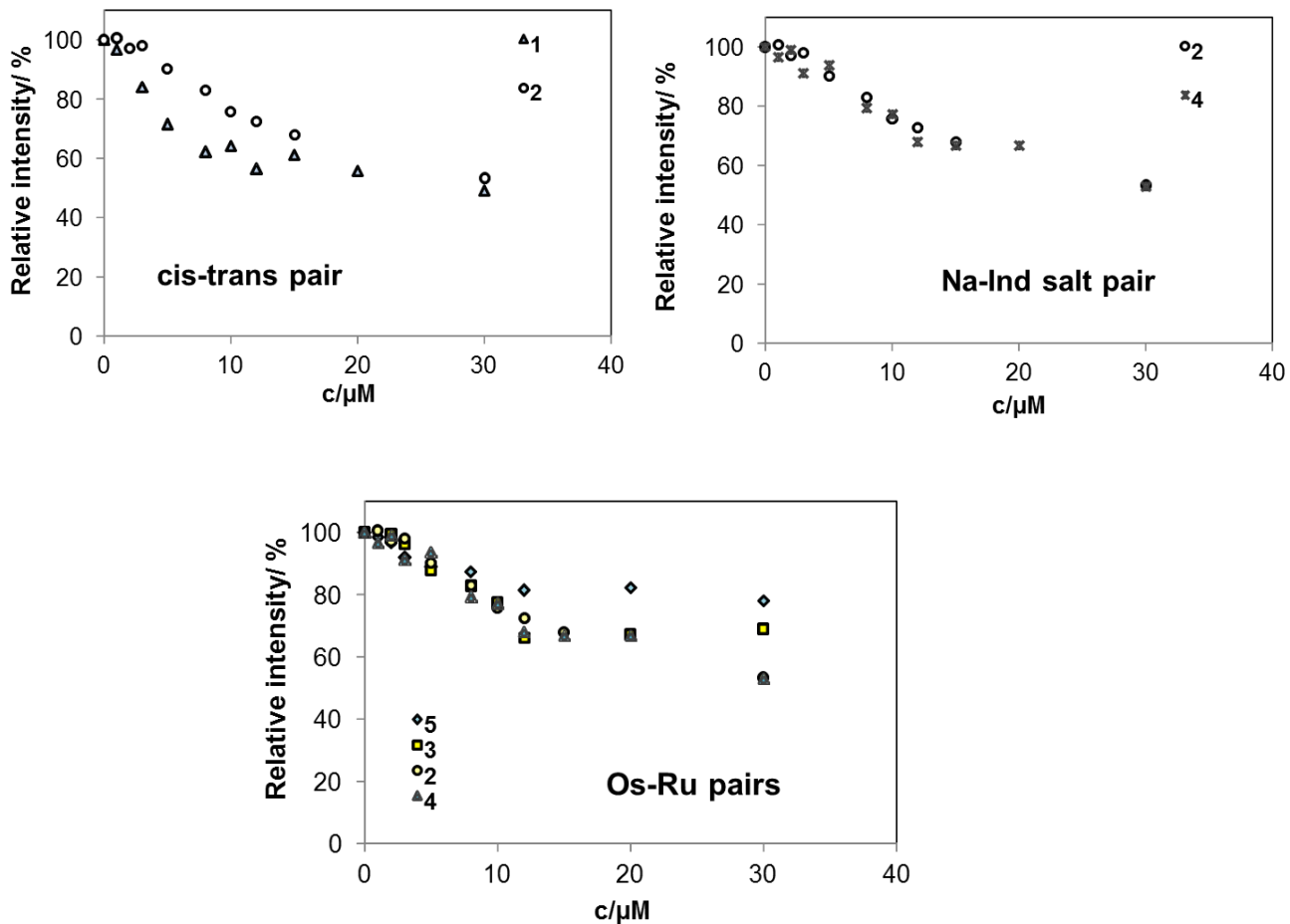
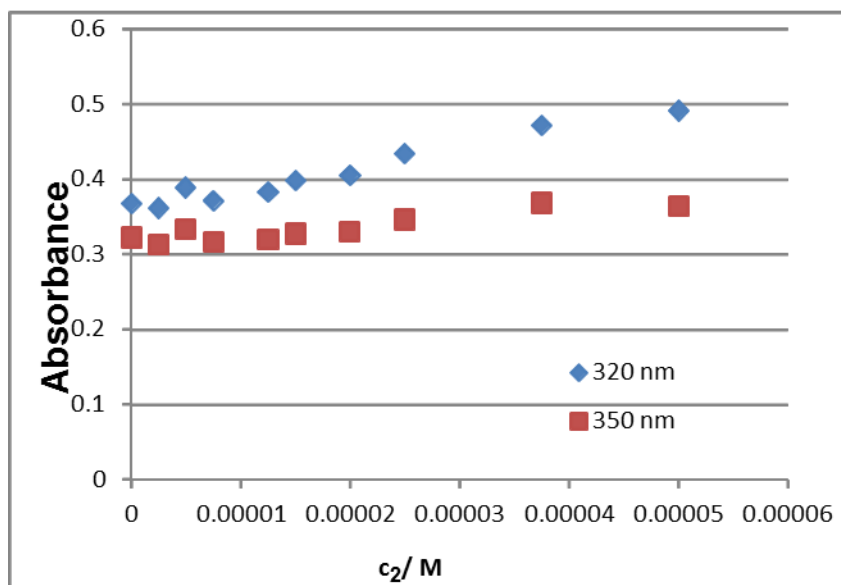


Figure 33. Intensities of DG emissions at 480 nm for various pairs of complexes.

The DG emission at 480 nm with increasing complex concentration was compared for the compounds Na[*cis*-OsCl₄NO(Hind)] (**1**), Na[*trans*-OsCl₄NO(Hind)] (**2**), the sodium (**2**) and the indazolium (**4**) salt of [*trans*-OsCl₄NOHind)] and for the Ru/Os pairs of (Hind) [*trans*-Ru(**5**)/Os(**4**)Cl₄NO(Hind)] and Na[*trans*-Ru(**3**)/Os(**2**)Cl₄NO(Hind)]. As expected from the logK' constants all compounds showed a very similar behavior (Fig. 33).

DTDP method: binding to Cys-34 SH. The interaction of free SH-group with DTDP generates a 2-TP colored product ($\lambda_{\max} = 340$ nm). If the complex, respectively the NO-ligand, interacts with the SH-group of HSA, then the later added DTDP can interact just with the remainder SH-groups. A negative saturation curve is expected at increasing

amount of complex to HSA. No interaction between HSA and **2** or **3** on Cys-34 were observed (Fig. 34).



-
- ¹ Jørgensen, C.K., *Coord. Chem. Review*, **1966**, 1, 164–178.
- ² Silverman, R.B. *Acc. Chem. Res.* **2009**, 42, 439–445.
- ³ Serli, B.; Zangrado, E.; Gianferrara, T.; Yellowlees, L.; Alessio, E. *Coord. Chem. Rev.* **2003**, 245, 73–83.
- ⁴⁴ Lang, D.R.; Davis, J.A.; Lopes, L.G.F.; Ferro, A.A.; Vasconcellos, L.C.G.; Franco, D.W.; Tfouni, E.; Wieraszko, A.; Clarke, M.J. *Inorg. Chem.* **2000**, 39, 2294–2300.
- ⁵ Kaneto, H.; Fujii, J.; Suzuki, K.; Matsuoka, T.; Nakamura, M.; Tasumi, H.; Kamada, T.; Taniguchi, N. *Diabetes*, **1995**, 44, 733–738.
- ⁶ Ho, Y.S.; Lec, H.H.; Mori, T.C.; Wong, Y.J.; Lin, J.K. *Mol. Carcinogenesis* **1997**, 19, 101–113.
- ⁷ (a) Messmer, U.K.; Reed, J.C.; Bruene, B. *J. Biol. Chem.* **1996**, 271, 20192–20197.
(b) Bruene, B.; Messmer, U.K.; Sandau, K. *Toxicol. Lett.* **1995**, 82/83, 233–237.
- ⁸ Slocik, J.M.; Shepherd, R.E. *Inorg. Chim. Acta* **2000**, 311, 80–94.
- ⁹ Slocik, J.M.; Ward, M.S.; Somayajula, K.V.; Shepherd, R.E. *Transition Met. Chem.* **2001**, 26, 351–364.
- ¹⁰ Coe, B.J.; Glenwright, S.J. *Coord. Chem, Review*, **2000**, 203, 5–80.
- ¹¹ Toshiyuki H.; Takao O.; Hirota N.; Keiji M. *Inorg. Chem.*, **2003**, 42, 6575–6576.
- ¹² Bučinský, L.; Büchel, G.; Ponec, R.; Rapta, P.; Breza, M.; Kožíšek, J.; Gall, M.; Biskupič, S.; Fronc, M.; Schiessl, K.; Cuzan, O.; Prodius, D.; Turta, C.; Shova, S.; Zajac, D.; Arion, V. *Eur. J. Inorg. Chem.*, **2013**, 2505–1519.
- ¹³ Prestaiko, A. W., Carter, S. K. *Academic Press: New York*, **1980**; 285–304.
- ¹⁴ Ishiyama T.; Matsumura T. *Bull. Chem. Soc. Jpn.*, **1979**, 52, 619–620.
- ¹⁵ Ishiyama T.; Matsumura T. *Annual Report of the Radiation Center of Osaka Prefecture*, **1980**, 21, 7–9.
- ¹⁶ Zangl, A.; Klufers, P.; Schaniel D.; Woike, T. *Dalton Trans.*, **2009**, 1034–1045.
- ¹⁷ Hirano, T.; Oi, T.; Nagao, H.; Morokuma, K., *Inorg. Chem.*, **2003**, 42, 6575–6583.
- ¹⁸ Sinitsyn, N.M.; Petrov, K.I. *Zhurnal Strukturnoi Khimii* **1968**, 9, 45–53.
- ¹⁹ Emel'yanov, V.; Baidina, A.; Khranenko, S.; Gromilov, S.; Il'in, M.; Belyaev, V. *J. of Struct. Chem.*, **2003**, 44, 37–45.

-
- ²⁰ Enyedy, E.; Hollender, D.; Kiss, T. *J. Pharm. Biomed. Anal.*, **2011**, *54*, 1073–1081.
- ²¹ *SAINT-Plus*, version 7.06a and APEX2; Bruker-Nonius AXS Inc.: Madison, WI, **2004**.
- ²² Sheldrick, G. M. *Acta Crystallogr. A* **2008**, *64*, 112–122
- ²³ Burnett, M.N.; Johnson, G. K. ORTEP. Report ORNL-6895. OAK Ridge National Laboratory; Tennessee, **1996**.
- ²⁴ Gavriluta, A.; Büchel, G.; Freitag, L.; Novitchi, G.; Tommasino, J.; Jeanneau, E.; Kuhn, P.; Gonzales, L.; Arion, V.; Luneau, D. *Inorg. Chem.*, **2013**, *52*, 6260–6272.
- ²⁵ Chasteen N.; Grady J.; Holloway C.; *Inorg Chem* , **1986**, *25*, 2754–2760.
- ²⁶ Ze'ka'ny, L.; Nagypa, I. In: Leggett DL (ed) *Computational methods for the determination of stability constants*. Plenum, New York, **1985**, 291–353.
- ²⁷ Lakowicz, J. *Principles of fluorescence spectroscopy, 3rd edn*. Springer, New York, **2006**.

Supplementary

Experimental 1

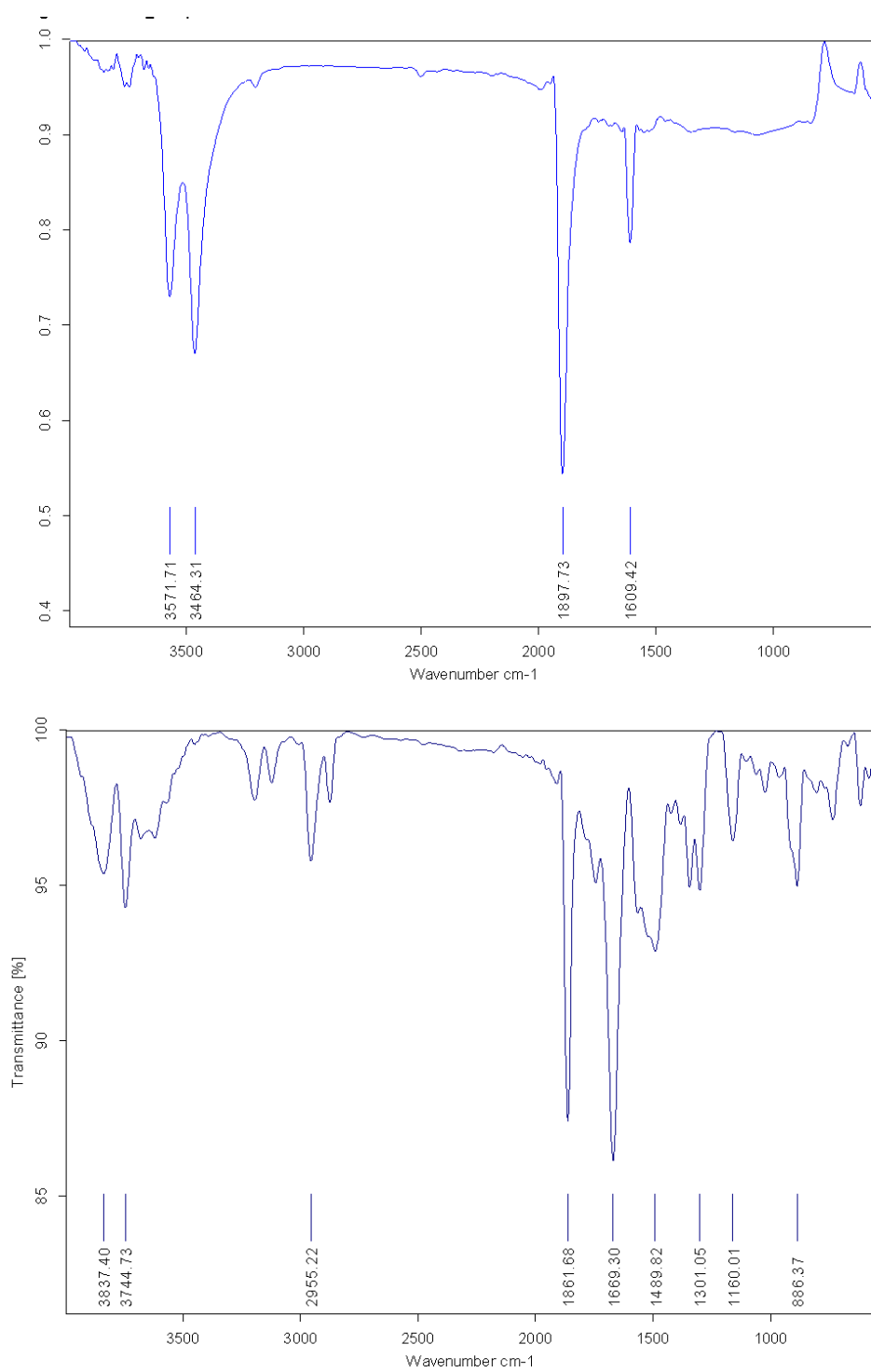


Figure S1. ATR-IR spectra of Na₂[RuCl₅NO]·6H₂O and **1**.

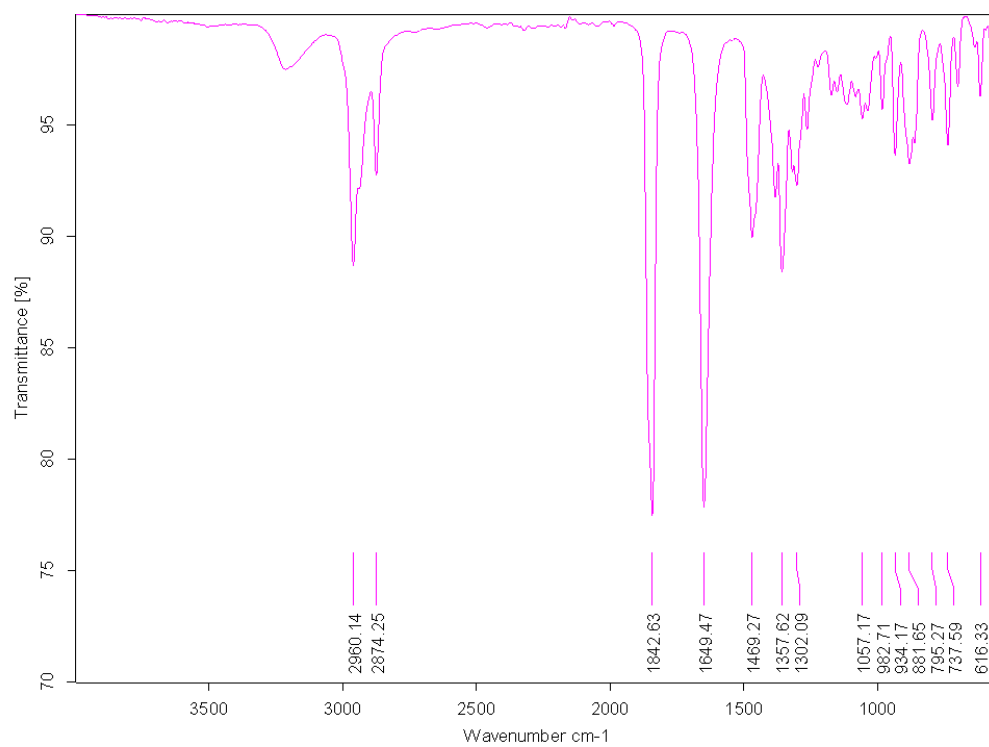
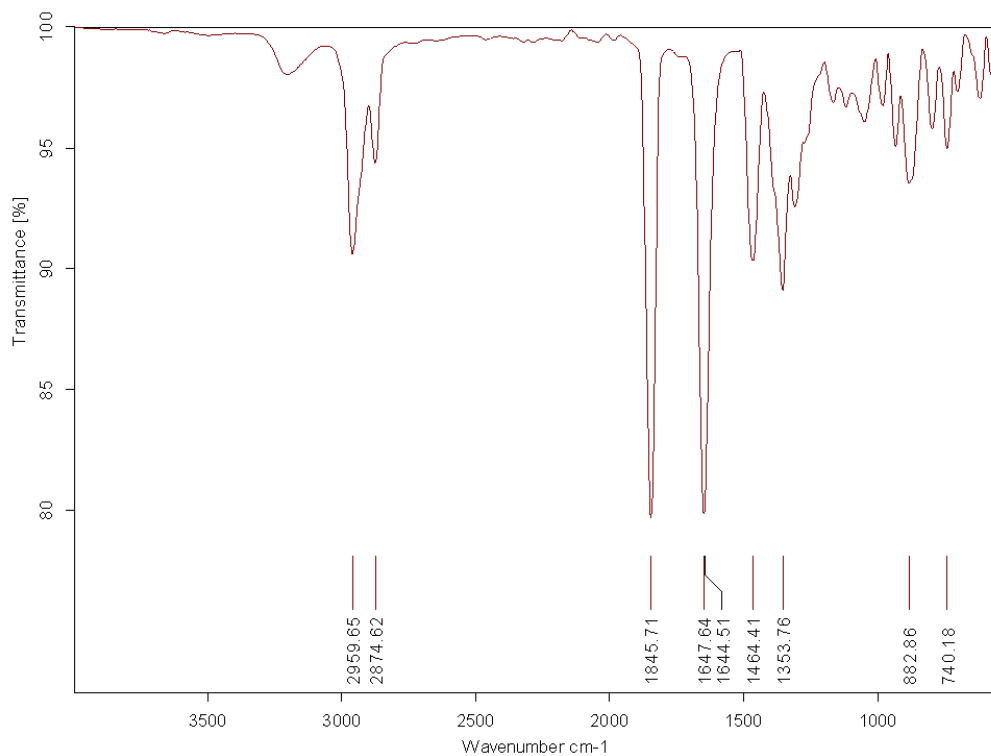


Figure S2. ATR-IR spectra of **2** and **3**.

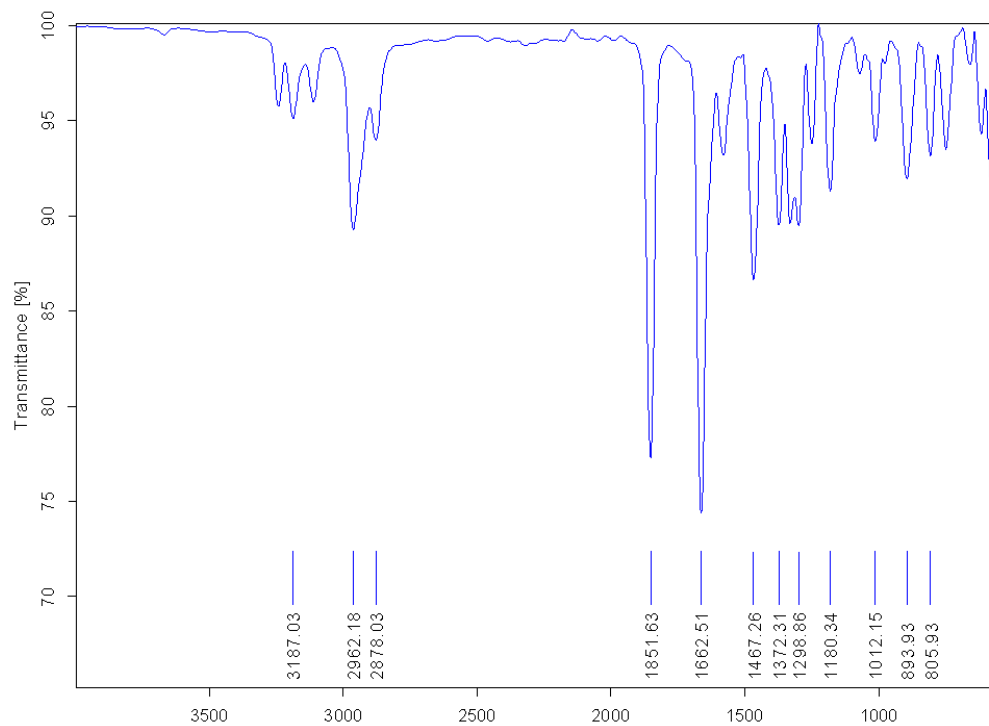
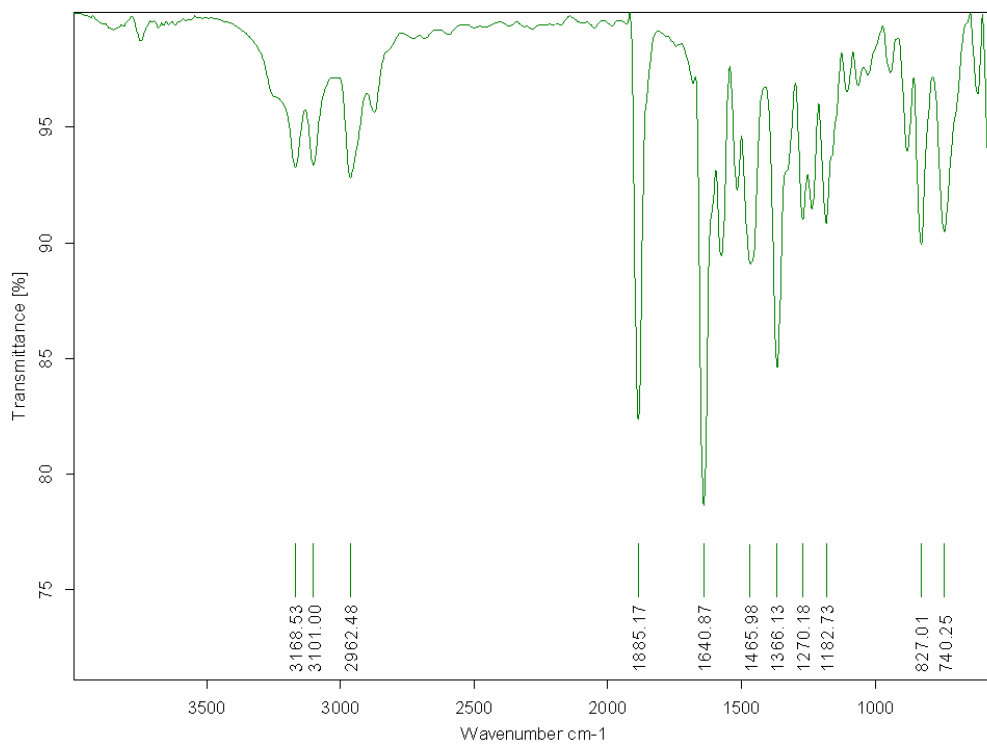


Figure S3. ATR-IR spectra of **4** and **5**.

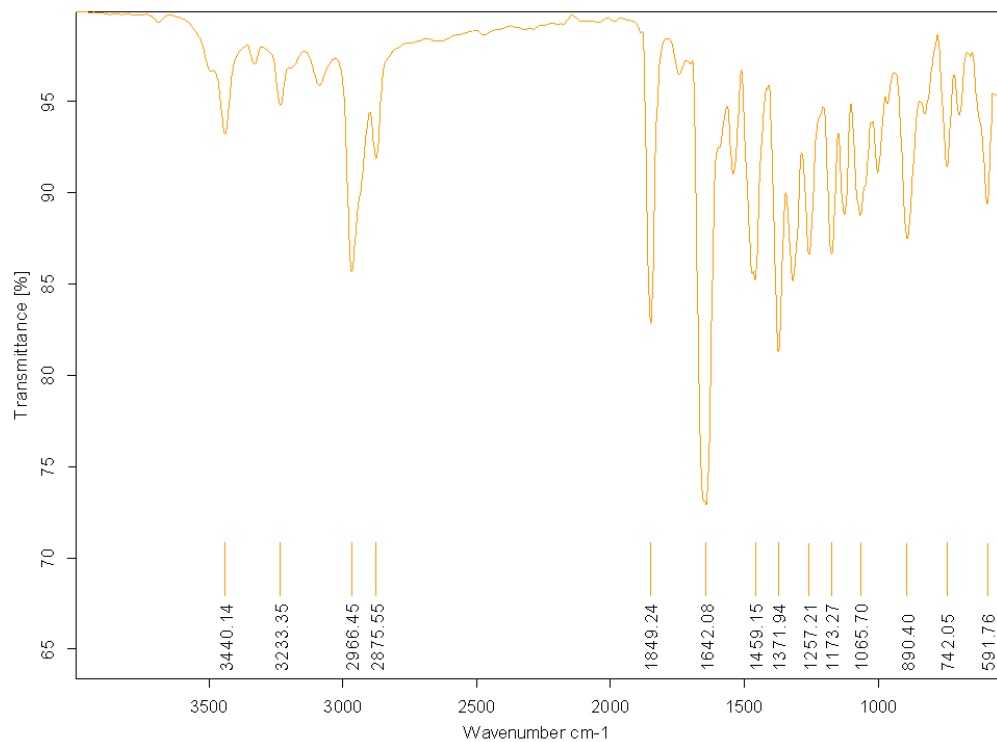
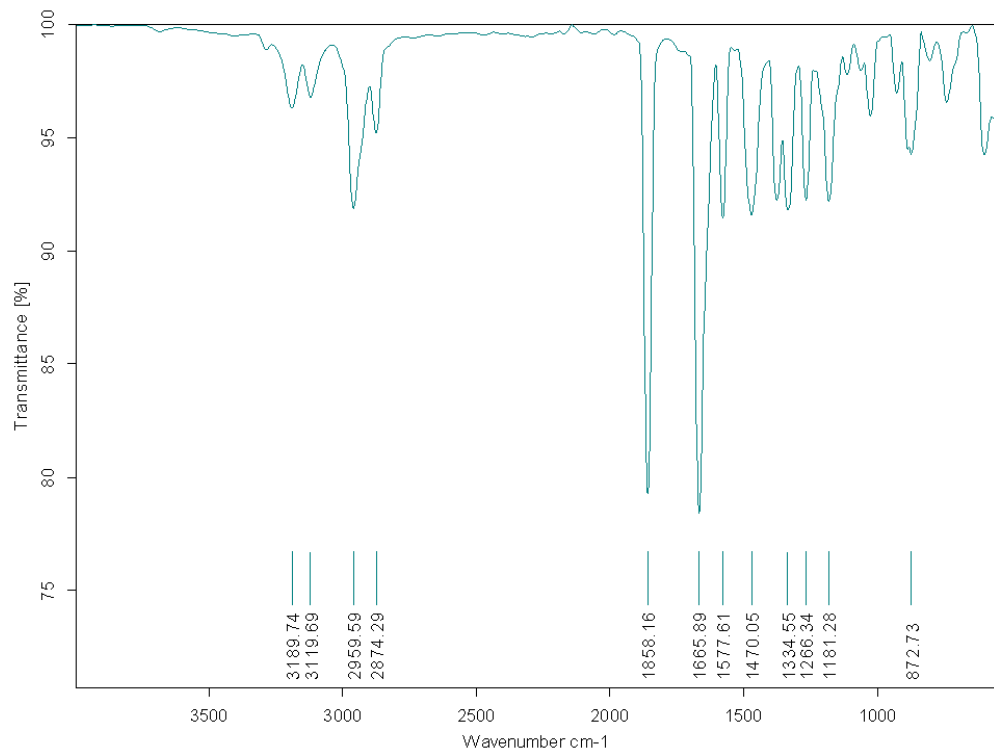


Figure S4. ATR-IR spectra of **6** and **7**.

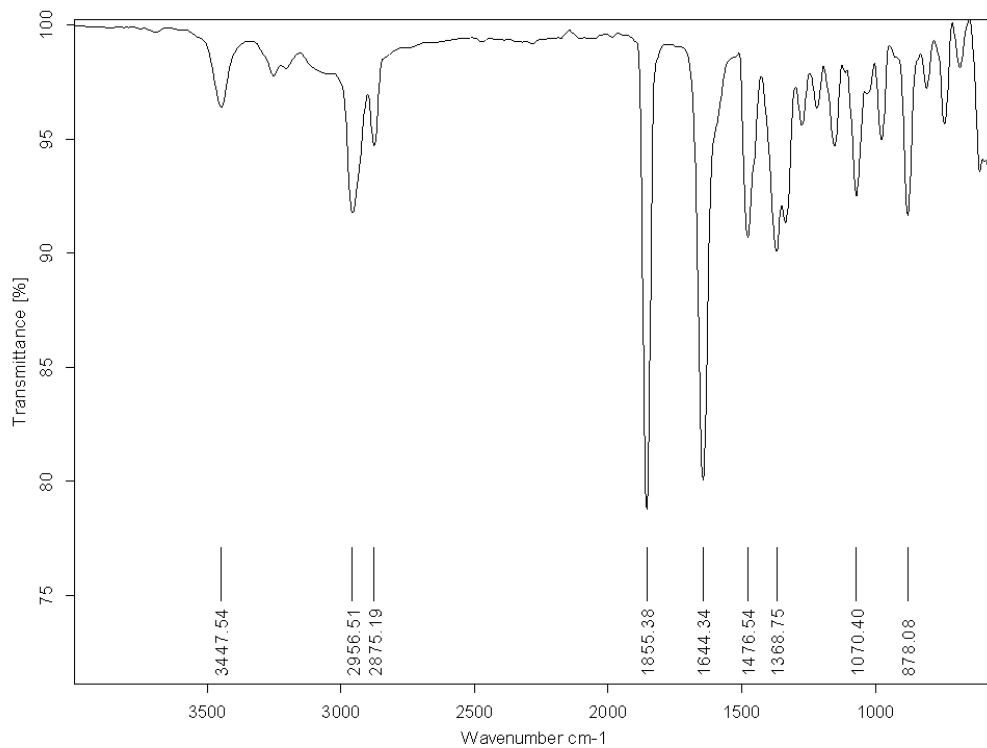


Figure S5. ATR-IR spectra of **8**.

Experimental 2

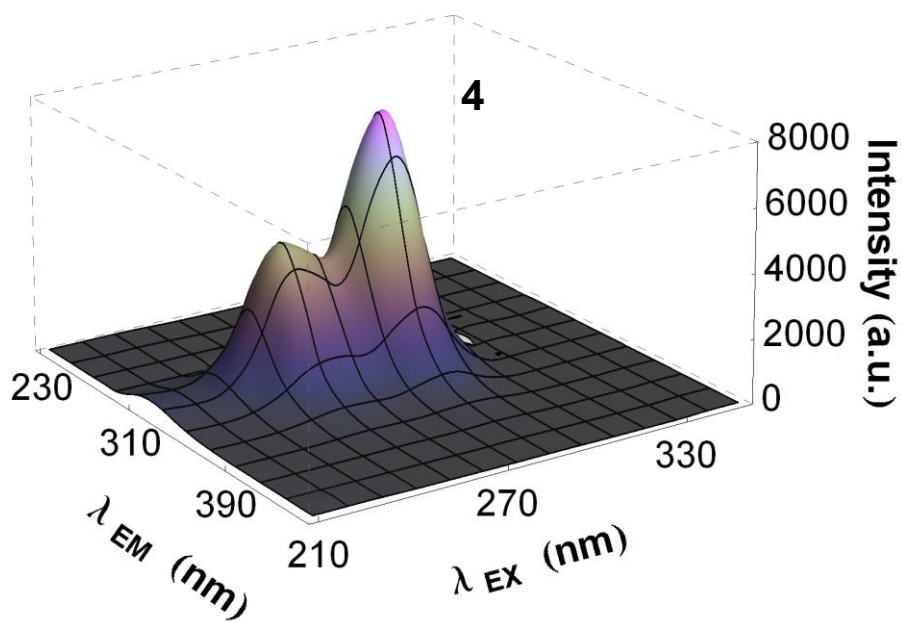


Figure S6: Excitation spectrum of $(H_2Ind)trans[RuCl_4NO(Hind)]$ (**4**) at 330 nm.

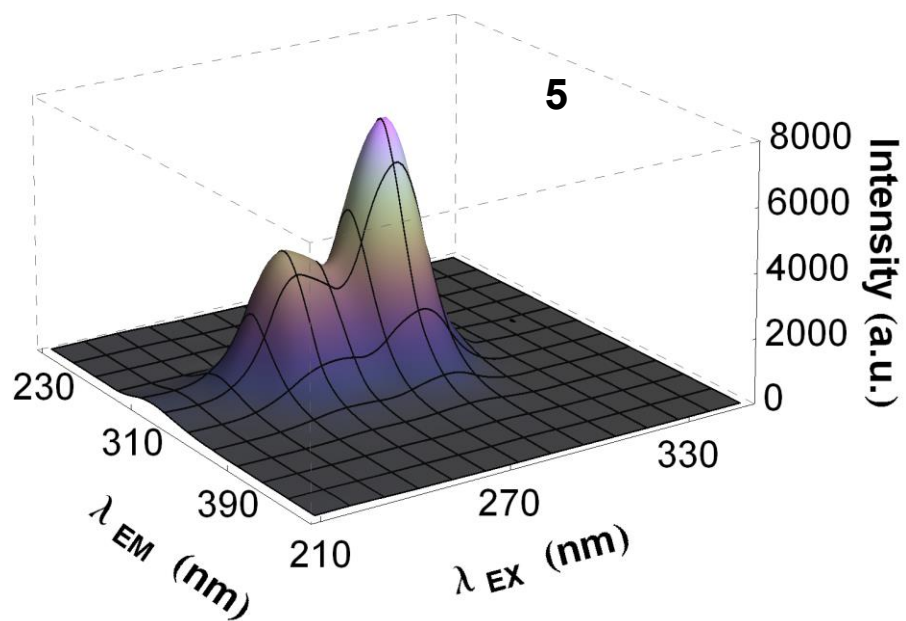


Figure S7: Excitation spectrum of $(H_2Ind)trans[OsCl_4NO(Hind)]$ (**5**) at 330 nm.

Curriculum vitae

Anna Rathgeb.

Education

03/2007 – until end of July 2013	studies of chemistry at the University of Vienna
10/2006 – 02/2007	studies of pharmacy (discontinued)
2004 – 2006	Akademisches Gymnasium Salzburg (High School)
1998 – 2004	Bundesgymnasium St. Johann im Pongau (High School)
1994 – 1998	Elementary School Schwarzach im Pongau

Previous research activity

Master thesis at the Institute of Inorganic Chemistry, Supervisor Prof. Arion

“Synthesis and Characterization of Ruthenium-Nitrosyl Complexes with Amino Acids” Starting from $\text{Na}_2[\text{RuCl}_5\text{NO}]$ various complexes of the general formula $(\text{Bu}_4\text{N})[\text{RuCl}_3\text{NO}/\text{D-AA}]$ were prepared and characterized by elemental analysis, ESI-MS, UV-vis, IR-spectroscopy and X-ray crystallography. IC_{50} values on three different human cancer cell lines were determined.

Research stay at the Department of Inorganic and Analytical Chemistry of the University of Szeged, Szeged, HU

The binding of $(\text{H}_2\text{Ind})/\text{Na} [\text{cis/trans-MCl}_4\text{NO}(\text{Hind})]$, $\text{M} = \text{Os}, \text{Ru}$, to HSA was investigated by UV-vis and fluorescence spectroscopy.

Bachelor thesis at the Institute of Inorganic Chemistry, Supervisor Prof. Arion

„Indolochinoline-aldehyde as Starting Compound for the Synthesis of New Anti-cancer Active Ruthenium Complexes“, The ligand system was synthesized and complexed with Ru₂Cl₄(p-cym)₂.

Teaching Experience

03/2013 supervision of a bachelor student in the framework of my mater thesis

Relevant Professional Experience

07/2010 internship at the Austrian Agenture for Health and Food Safety (AGES)

Research Skills

- Analytical HPLC
- 1D and 2D NMR spectra interpretation
- ESI MS
- UV-vis and IR spectroscopy
- Basic knowledge in x-ray diffractometry

Other Qualifications

Languages English, fluent; German, native tongue; basic French

Programms MS Office, high level of user skills

Personal Qualities:

Reliable, accurate, able to work in a team, eager to learn, humorous

Intrests:

Dancing, literature, cooking